Journal of Mammalian Evolution
https://doi.org/10.1007/s10914-022-09636-2

ORIGINAL PAPER

A new multituberculate from the latest Cretaceous of central China and its implications for multituberculate tooth homologies and occlusion

Xingsheng Jin[1] · Fangyuan Mao[2,3] · Tianming Du[1] · Yihan Yang[2,4] · Jin Meng[3,5]

Accepted: 27 September 2022

Abstract

Cimolodontan multituberculates are common in the Late Cretaceous and Paleocene of central Asia; they are rarely known from regions south of the Mongolian plateau. Here, we report a new genus and species of multituberculate, *Erythrobaatar ganensis* gen. et sp. nov., from the Late Cretaceous of Ganzhou, Jiangxi Province, central China, representing the southernmost record of Cretaceous multituberculates in Eurasia. The new species is based on two well-preserved specimens that include cranial and postcranial materials. With a cranium and dentary length of 83 and 66 mm, respectively; it is one of the largest known Cretaceous multituberculates from Eurasia. The present work focuses on the description of the craniodental morphology of the new species, in comparison with that of other Late Cretaceous and Paleogene cimolodontans in order to establish the new taxon. *Erythrobaatar ganensis* is most closely related to *Yubaatar zhongyuanensis* and *Yubaatar qianzhouensis* in the shape and size of the skull and teeth. Phylogenetic analyses place the new species within Taeniolabidoidea, which consists mostly of Late Cretaceous and Paleogene cimolodontans from Asia and North America. The new material also sheds light on tooth replacement, reduction, homologies, and occlusion of multituberculates with a focus on cimolodontans.

Keywords Mammalia · Multituberculata · Cimolodonta · Late Cretaceous · Central China · Ganzhou Basin

Introduction

Multituberculates are the most diverse Mesozoic mammals (Kielan-Jaworowska et al. 2004; Weil and Krause 2008) with the longest geological distribution in mammals, from at least the Middle Jurassic (Butler and Hooker 2005; Averianov et al. 2021) to the late Eocene (Krishtalka et al. 1982; Swisher and Prothero 1990). Cimolodonta were a relatively derived group of multituberculates that contains some Early Cretaceous and nearly all Late Cretaceous and Paleogene species (Kielan-Jaworowska et al. 2004). Some of them are represented by complete skulls and even postcranial skeletal materials from Europe, North America, and Asia (mainly Mongolia and China) (e.g., Gidley 1909; Sloan 1979; Krause 1982; Kielan-Jaworska et al. 1987; Miao 1988; Novacek et al. 1994; Rădulescu and Samson 1996; Kielan-Jaworowska and Hurum 1997; Weil and Tomida 2001; Fox 2005; Smith and Codrea 2015; Csiki-Sava et al. 2018; Hu and Han 2021; Krause et al. 2021; Weaver et al. 2021). Cimolodontans were one of few clades of mammals that survived the Cretaceous-Paleogene (K-Pg) extinction event, and although many lineages went extinct, the group as a

Xingsheng Jin and Fangyuan Mao authors contributed equally to this work.

✉ Fangyuan Mao
maofangyuan@ivpp.ac.cn

✉ Jin Meng
jmeng@amnh.org

1 Zhejiang Museum of Natural History, Zhejiang Province, Hangzhou 310014, China

2 Key Laboratory of Evolutionary Systematics of Vertebrates, Institute of Vertebrate Paleontology and Paleoanthropology, Chinese Academy of Sciences, Beijing 100044, China

3 Division of Paleontology, American Museum of Natural History, New York, NY 10024, USA

4 School of Earth Sciences, China University of Geosciences, Wuhan 430074, China

5 Earth and Environmental Sciences, Graduate Center, City University of New York, New York, NY 10016, USA

Published online: 27 October 2022

whole remained diverse, abundant, and increased in dental complexity and body size disparity across the K-Pg boundary (Wilson et al. 2012).

The Late Cretaceous and Paleogene cimolodontans from Eurasia are best known from the Mongolian plateau (Kielan-Jaworowska et al. 2004). South of the Mongolian plateau, multituberculates were only reported from the Lower Eocene of the Wutu Basin, Shandong Province in east China (Tong and Wang 2006), the Upper Cretaceous of Luanchuan, Henan Province in the middle of China (Xu et al. 2015), and the Upper Cretaceous of Ganzhou, Jiangxi Province, central China (Hu and Han 2021). Here, we report another new genus and species of cimolodontan multituberculate from the Upper Cretaceous of Ganzhou, Jiangxi Province, China. The new taxon is based on two well-preserved specimens with craniodental and postcranial remains. The materials from Ganzhou are the southernmost known record of Cretaceous multituberculates in East Asia. The new species represented is one of the largest Late Cretaceous multituberculates in Eurasia. This record adds to the diversity of Late Cretaceous multituberculates of Asia and lends support to the view that there was an adaptive radiation of multituberculates that began before the K-Pg extinction and that disparity in dental complexity and body size rose sharply during the latest Cretaceous (Wilson et al. 2012). We provide a brief description of the craniodental morphologies to establish the new genus and species and take the opportunity to discuss some outstanding issues in multituberculate evolution, including upper fourth premolar homology, reduction of mesial upper premolars and resulting issues of homology, and tooth occlusion of multituberculates when the dentition is considered as a whole.

Geological setting

The holotype and paratype specimens of *Erythrobaatar ganensis* were collected from the Upper Cretaceous Hekou Formation of Nanxiong Group, Ganzhou City, Jiangxi Province, Central China (Fig. 1) from sites that were exposed by construction activities associated with local infrastructure development. The holotype specimen (GM30516) of *Erythrobaatar ganensis* came from the site of Ganzhou railway station, east of Ganzhou City, which is the same site as the holotype of the oviraptorid *Huanansaurus ganzhouensis* (see Lü et al. 2015). The paratype specimen (GM30496) of *E. ganensis* was excavated from a site near the Third High School of Ganxian, northeast of Ganzhou City, where the holotype specimen of oviraptorid *Tongtianlong limosus* (see Lü et al. 2016) was discovered. The recently reported holotype specimen of *Yubaatar qianzhouensis* (Hu and Han 2021) also came from the Hekou Formation of the Ganxian development zone, but no specific locality was identified.

The Ganzhou Basin is located in the southern part of Jiangxi Province; it is northeast-southwest extended and has an area of about 1200 km^2. Strata of red mudstones, sandstones, and conglomerates exposed in this basin are mainly Late Cretaceous in age and had been generally identified as consisting of the lower Ganzhou Formation and the upper Nanxiong Formation (Bureau of Geology and Mineral Resources of Jiangxi Province 1984). In more recent studies, ranging from bottom-up, the strata were subdivided into the Maodian Formation and Zhoutian Formation of the Ganzhou Group (=Ganzhou Formation), and the Hekou Formation, Tangbian Formation, and Lianhe Formation of the Guifeng Group (=Nanxiong Formation), respectively (Liu 1997). The vertebrate fossil sites are in the NE-SW extended, fan-shaped Gannan Basin, located in the central west of Ganzhou Basin and around Ganzhou City. In this area, only the Maodian, Zhoutian, and Hekou formations crop out (Fig. 1). The lower Maodian Formation has yielded an assemblage, consisting mainly of eggs that were well preserved and laid elaborately in circular nests. These dinosaurian eggs belong to *Spheroolithus spheroids*, *Macroolithus rugustus*, and *Elongatoolithus elongatus* (Zhao, 1975, 1979; Bureau of Geology and Mineral Resources of Jiangxi Province 1984; Liu 1999; Lucas 2001). Except for those laid in nests (Young 1965), some eggs from Hekou Formation were found associated with bones, inside the female adult pelvis or even embryo-bearing (Sato et al. 2005; Cheng et al. 2008; Wang et al. 2016; Jin et al. 2020; Xing et al. 2021). No fossil has been reported from the Zhoutian Formation in this area until now.

Vertebrate fossils were also reported from the Nanxiong Formation (=Guifeng Group) that is exposed in the vicinity of the Gannan Basin; these fossils include the oviraptorids *Banji long* Xu and Han, 2010, *Ganzhousaurus nankangensis* Wang et al., 2013, *Jiangxisaurus ganzhouensis* Wei et al., 2013, *Nankangia jiangxiensis* Lü et al., 2013a, *Huanansaurus ganzhouensis* Lü et al., 2015, and *Tongtianlong limosus* Lü et al., 2016; the tyrannosaurids *Qianzhousaurus sinensis* Lü et al., 2014 and *Gannansaurus sinesis* Lü et al., 2013b; the titanosaurian *Titanosaurus* sp. (Bureau of Geology and Mineral Resources of Jiangxi Province 1984); isolated theropod teeth (Mo and Xu 2015); the squamates *Conicodontosaurus kanhsienensis* Young, 1973, *Tianyusaurus zhengi* Lü et al., 2008 (Mo et al. 2010), and *Chianghsia nankangensis* Mo et al., 2012; and the turtles ?*Nanhsiungchelys* sp. (Bureau of Geology and Mineral Resources of Jiangxi Province 1984), *Jiangxichelys ganzhouensis* Tong and Mo, 2010, and *Jiangxisuchus nankangensis* Li et al., 2019. Most of these fossils were collected by local farmers and exposed from localities around Nankang District, Longling town, the Ganzhou

Fig. 1 Geographic map showing the distribution of the Upper Cretaceous strata and main vertebrate fossil localities in southern Ganzhou Basin (based on He et al. 2017 and Bureau of Geology and Mineral Resources of Jiangxi Province 1984). The lower mammal site is the site of Ganzhou railway station, where the holotype (GM30516) of *Erythrobaatar ganensis* came from; the upper mammal site is the site of the Third High School of Ganxian, where the paratype (GM30496) of *Erythrobaatar ganensis* was uncovered. Scale bar equals 5 km

railway station, the Third High School of Ganxian County, and Miaodian Town; their exact stratigraphic positions and correlations need more investigation. However, if the result of the geological survey is correct (Bureau of Geology and Mineral Resources of Jiangxi Province 1984; Liu 1997), the strata of all the localities mentioned above should belong to the Hekou Formation, Guifeng Group (Fig. 1).

By biostratigraphic correlation, the ages of the Maodian and Hekou formations were estimated as Campanian

and Maastrichtian, respectively (Zhao et al. 1991; Lucas 2001; Sato et al. 2005; He et al. 2017). These age estimates have been supported by radioisotopic dating of the basalt-pyroclastic-sedimentary rocks within the Maodian Formation (Zhong et al. 2002). In comparison with other Late Cretaceous multituberculates, such as *Yubaatar zhongyuanensis* (Xu et al. 2015), and viewed within the general evolutionary stages of multituberculates, the large size and some advanced morphological features of the new species appear consistent with the age estimates.

Materials and methods

The specimens (GM30516 and GM30496) include cranial and partial postcranial remains from two individuals and are housed in the Zhejiang Museum of Natural History, Hangzhou, Zhejiang Province China.

Anatomical terminologies follow Wible and Rougier (2000), Rougier et al. (2016) and Wible et al. (2019) for the skull, and Kielan-Jaworowska et al. (2004) for the dentition.

Optical images were taken using a Canon Digital camera with a macro lens installed in the Key Laboratory of Vertebrate Evolution and Human Origins, Institute of Vertebrate Paleontology and Paleoanthropology (IVPP), Chinese Academy of Sciences.

High-resolution micro-CT scanning of both specimens of *Erythrobaatar ganensis* (GM30516 and GM30496) was conducted using a GE v|tome|x m dual tube 240/180 kV system in the Institute of Vertebrate Paleontology and Paleoanthropology, Chinese Academy of Sciences (IVPP). Specimens were scanned using the 240kv microfocus tube at 15–56 microns/voxel resolution, 120–260 kV and 150–200 µa. Where needed, a 0.1 mm Cu filter was used to reduce beam hardening artifacts. To improve the signal-to-noise ratio, 1800 projections were collected, for 333–2000 ms and averaged 2–3 times. To accommodate the long holotype (GM30516), two scans for two separate portions of the cranium in the Y-axis (multiscan) were conducted to obtain higher resolution. The scan data were reconstructed using Phoenix datos|x (General Electric, Wunstorf, Germany). Segmentation and the rendering of the CT scanning data were processed using VGStudio Max 3.5 (Volume Graphics, Heidelberg, Germany).

Measurements were taken using digital calipers to two decimal digits and double-checked using digital methods from the images. After these elements were reconstructed, linear measurements were taken using the Measurements Menu/Coordinate Measurement module in VGStudio Max 3.5 (Volume Graphics, Heidelberg, Germany) and rechecked using the measurement tool in ImageJ 1.49v.

We used two data matrices in our phylogenetic analyses. Dataset I is modified from Wible et al. (2019), which includes most Late Cretaceous Mongolian multituberculate species that are represented by relatively well-preserved cranial material. This data matrix sampled taxa and characters used in several previous studies on phylogenetic relationships of the Late Cretaceous Mongolian multituberculates (Simmons 1993; Kielan-Jaworowska and Hurum 1997; Rougier et al. 1997, 2016). We modified this dataset by adding two taxa, *Yubaatar zhongyuanensis* (Xu et al. 2015) and *Erythrobaatar ganensis* (this study), and 47 craniodental characters that are derived from previous studies (Mao et al. 2016; Csiki-Sava et al. 2018; Wang et al. 2019). The characters are briefly listed in the Online Resouce 1. Thus, our updated data matrix contains 20 multituberculates and 121 characters.

Dataset II is modified from Smith et al. (2022), which was also based on several previous studies (Rougier et al. 1997; Weil 1998; Kielan-Jaworowska and Hurum 2001; Luo et al. 2002; Cifelli et al. 2013; Yuan et al. 2013; Xu et al. 2015; Mao et al. 2016; Csiki-Sava et al. 2018; Wang et al. 2019; Kusuhashi et al. 2020; Weaver et al. 2021). Most taxa selected in this matrix are at the generic level, except *Kogaionon*, *Hainina*, *Barbatodon*, *Yubaatar*, and *Erythrobaatar*. We use this data matrix to run phylogenetic analyses to identify the relationship of the new taxon within a broader sample of multituberculates with some non-multituberculate clades. The dataset includes 57 taxa and 130 characters; we added *Erythrobaatar ganensis* and *Yubaatar qianzhouensis* (Hu and Han 2021) and modified some coding of *Sinobataar*, *Yubaatar zhongyuanensis*, *Lambdopsalis*, *Spenopsalis*, and *Taeniolabis*.

The phylogenetic analyses were performed using PAUP Version 4.0a (Swofford 2002), random addition sequence 1,000 replications, 10 trees held at each step, tree-bisection-reconnection (TBR) branch-swapping algorithm with reconnection limit of eight, steepest descent option not in effect, initial 'Maxtrees' setting of 10,000, and 'MulTrees' option not in effect. As Smith et al. (2022), we considered 17 characters (characters 17, 25, 26, 29, 31, 32, 43, 46, 47, 49, 51, 52, 58, 59, 61, 72, 85) for the dataset II ordered, and the others unordered. All characters were equally weighted. A heuristic search criterion was conducted and no outgroup taxon was designated in either data analysis.

Abbreviations **d**, deciduous; **I**, upper incisor; **i**, lower incisor; **L**, left; **M**, upper molar; **m**, lower molar; **P**, upper premolar; **p**, lower premolar; **R**, right.

Institutional abbreviations **AMNH**, American Museum of Natural History, New York, New York; **BPMC**, Beipiao Pterosaur Museum of China, Chaoyang, Liaoning Province, China; **DMNH**, Denver Museum of Nature & Science, Denver, Colorado; **GM**, Zhejiang Museum of Natural History, Hangzhou, Zhejiang Province, China; HIII, Henan Geological

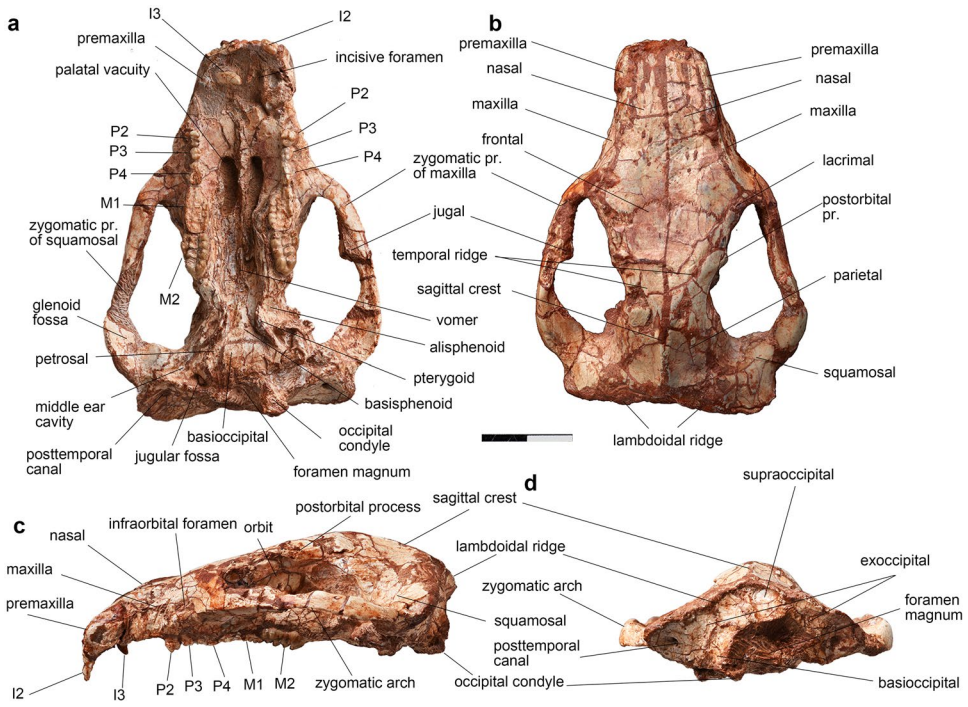

Museum, Zhengzhou, Henan Province, China; **IVPP**, Institute of Vertebrate Paleontology and Paleoanthropology, Chinese Academy of Sciences, Beijing, China; **USNM**, United States National Museum, Washington D.C., USA.

Systematic paleontology

Mammalia Linnaeus, 1758
Allotheria Marsh, 1880
Multituberculata Cope, 1884
Cimolodonta McKenna, 1975
Taeniolabidoidea Sloan and Van Valen, 1965
Erythrobaatar gen. nov.
Figures 2, 3, 4, 5 and 6
ZooBank number: LSIDurn:lsid:zoobank.org:act:61FA2D83-010D-4747-AD6F-2DAAEC8DED7A.

Type species: *Erythrobaatar ganensis*.
Included species: The type species only.
Etymology: "*Erythro-*" (Latin), red, reddish, referring to the color of the type specimens; "-baatar", hero in Mongolian, a common suffix for generic names of cimolodontan multituberculates.

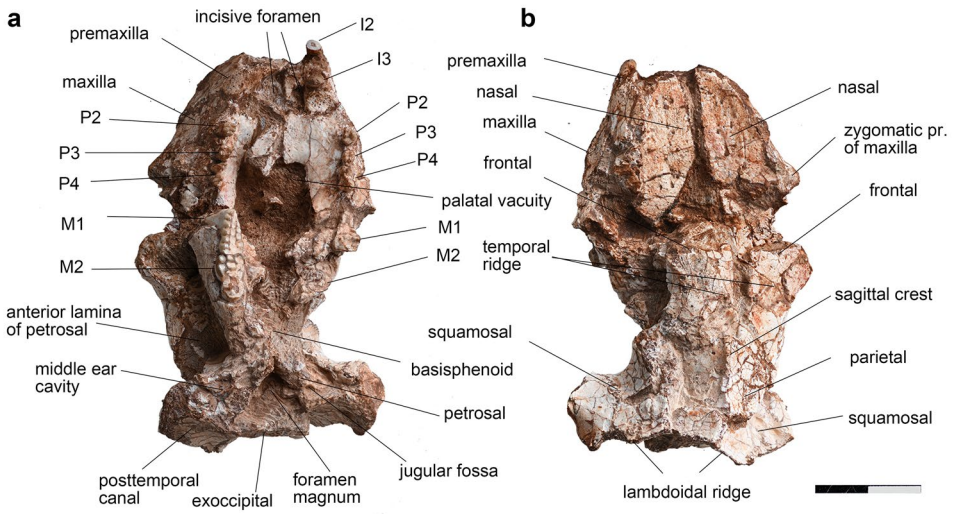

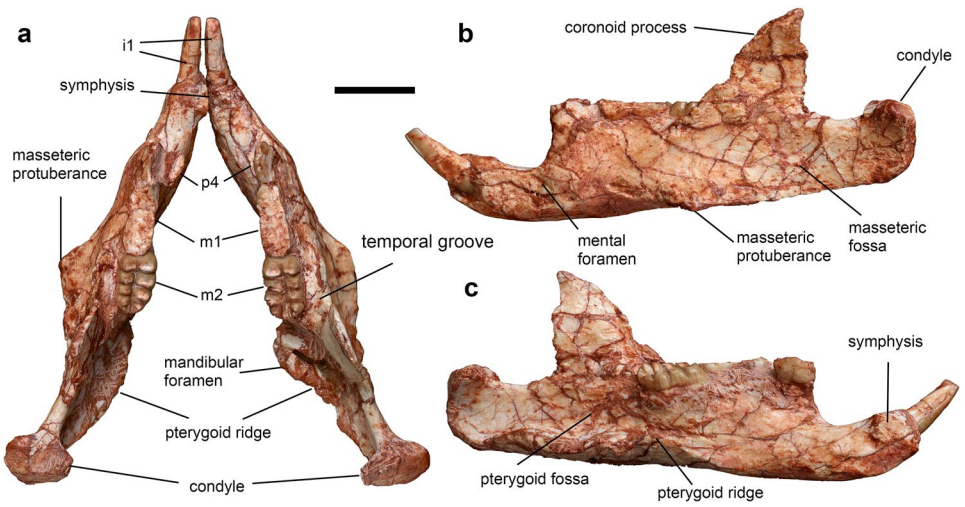

Fig. 4 Mandible of *Erythrobaatar ganensis* gen. et sp nov. (holotype, GM30516). **a**. dorsal view of the both dentaries; **b**. buccal view of left dentary; **c**. lingual view of left dentary. Scale bar equals 10 mm

Diagnosis: One of the largest known Mesozoic multituberculates in Eurasia with a cranium length = 83 mm, dentary length = 66 mm, and M1-2 length = 19.98 mm. *Erythrobaatar* differs from other multituberculates in having the following combination of features: dental formula 2:0:3:2/1:0:1:2; two single-cusped upper incisors that are robust and subequal in size; alveolus for I3 formed exclusively by premaxilla; long diastema between I3 and P2; cheek teeth lacking cusp ornamentation and coalescence; P4 is hourglass-shaped; cheek tooth cusp formulae P2(1–3:2–3), P3(2:2–3), P4(3:2?), M1(7:7:5–6), M2(2–3:4:4), p4(4), m1(7?:8?), m2(5–6:4–5); snout relatively long comparing to cranium; slender zygomatic arches with the anterior part directed transversely for a short distance and then immediately turning posterolaterally; single pair of long palatal vacuities; several dispersed vascular foramina on the nasals; frontals having a m-shaped anterior process that inserts between the nasals; small postorbital process immediately posterior to large lacrimal; ear region of braincase relatively short and even; nuchal crest posteriorly expanded; body (horizontal ramus) of dentary remarkably long but relatively shadow in depth and having flat ventral border; ventral border of dentary nearly parallel to occlusal plane; mandibular condyle placed at level of molars and facing dorsally; pterygoid ridge robust and labially extended. See Comparison for additional differences between *Erythrobaatar* and *Yubaatar* and other multituberculates.

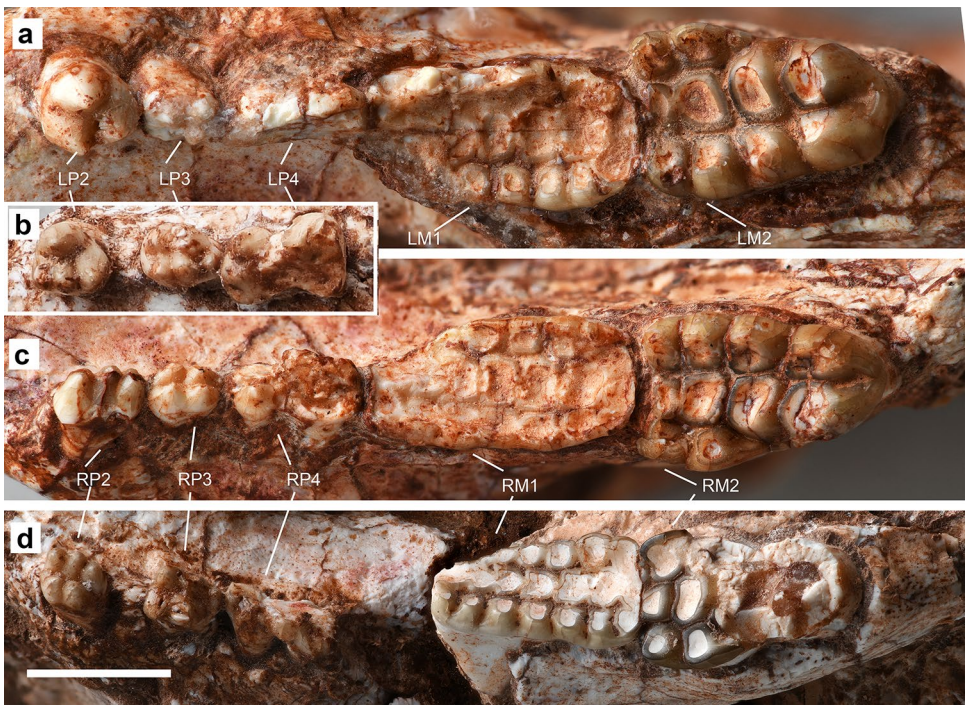

Fig. 5 Upper cheek teeth of *Erythrobaatar ganensis* gen. et sp nov. Left (**a**, **b**) and right (**c**, **d**) cheek teeth of holotype specimen GM30516 (**a**, **c**) and paratype specimen GM30496 (**b**, **d**). Abbreviations: **L**, left; **M**, upper molar; **P**, upper premolar; **R**, right. Scale bar equals 5 mm

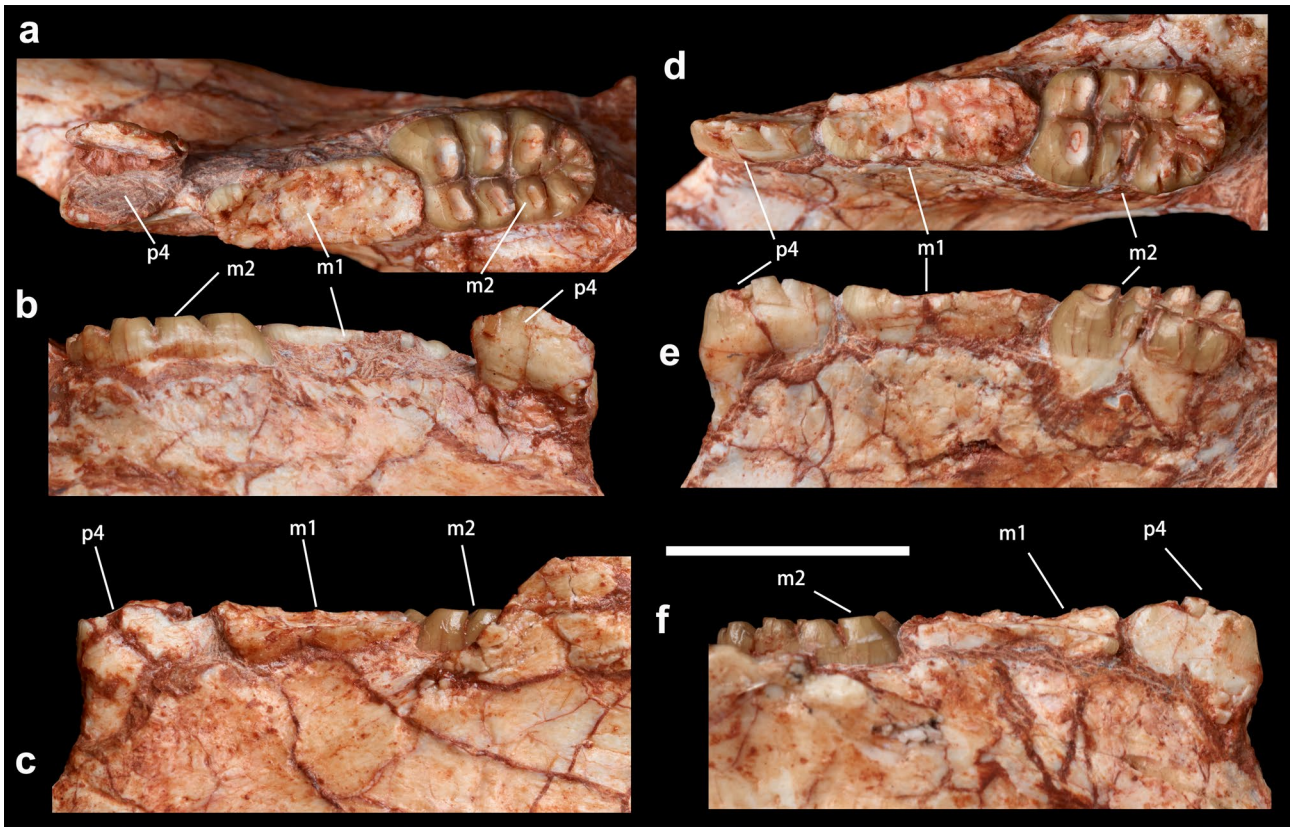

Fig. 6 Lower cheek teeth of *Erythrobaatar ganensis* gen. and sp. nov. (holotype, GM30516). Left (**a**-**c**) and right (**d**-**e**) sides of the cheek teeth in occlusal (**a**, **d**), lingual (**b**, **e**) and buccal (**c**, **f**) views. Abbreviations: **m**, lower molar; **p**, lower premolar. Scale bar equals 10 mm

Erythrobaatar ganensis gen. et sp. nov

ZooBank number: LSIDurn:lsid:zoobank.org:act:446F2111-B71C-4C09-A283-77411C66AA9E
Figs. 2, 3, 4, 5, 6 and 7c

Diagnosis: Same as the genus.

Etymology: "gan", pinyin spelling of Chinese character that is the short form for Ganzhou Province.

Holotype: Partial skeleton with a nearly complete cranium and both nearly complete dentary bones with the tip of coronoid process broken, and some postcranial elements including incomplete right forelimb, left and right hind limbs, and some vertebrae and ribs (GM30516, Zhejiang Museum of Natural History, Hangzhou, Zhejiang Province; Figs. 2, 4, 5 and 6).

Paratype: Distorted, partial cranium (GM30496, Zhejiang Museum of Natural History, Hangzhou, Zhejiang Province; Figs. 3 and 5).

Locality and Horizon: Ganzhou railway station (GM30516) and Third High School of Ganxian County (GM30496); Hekou Formation (Upper Cretaceous, Maastrichtian), Guifeng Group, Ganzhou City, Jiangxi Province, China.

Description

Cranial morphology The cranium of the holotype specimen (GM30516) of *Erythrobaatar ganensis* is nearly complete, well preserved, and only slightly distorted (e.g., plastic deformation on the right zygoma, obliquely distorted on the snout); only the anterior tip of the rostrum, the palatal area and the occipital condyles are slightly broken (Fig. 2). The paratype is poorly preserved such that the cranium was compressed in dorsoventrally and obliquely, and distorted with various parts missing (Fig. 3). The description of the cranium is largely based on the holotype. The profile of the cranium is slightly anteroposteriorly longer compared to those of other cimolodontans. In dorsal view, the nasal is long and gradually widens posteriorly, with the widest point at the nasal-lacrimal-maxilla junction. It sutures with the premaxilla and maxilla laterally, the lacrimal posterolaterally, and the frontal posteriorly. There are at least six foramina in the anterior two-thirds of each nasal that are arranged asymmetrically. The frontal is wedge-shaped with its broad anterior edge joining the nasals in an anteriorly convex, strongly interdigitated suture. Posteriorly, the frontals wedge deeply between the parietals to a point level with the anterior edge of the posterior root of the zygomatic arch. The parietal has an anterior

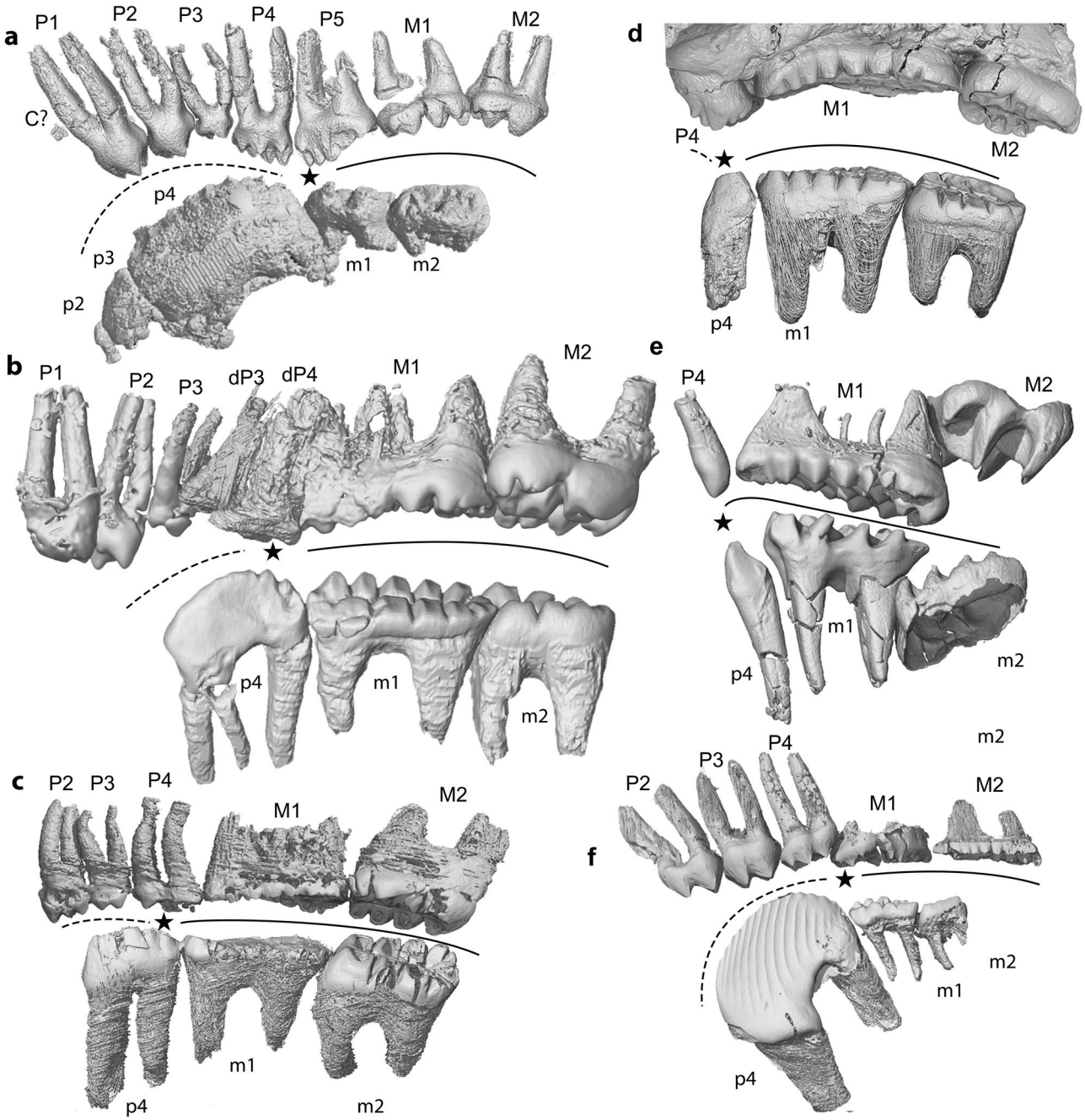

Fig. 7 Comparison of occlusal cycles in lateral views of the left upper and lower cheek teeth in selected multituberculates. **a**. *Sinobaatar pani* (upper cheek teeth, BPMC 0051, the Beipiao Pterosaur Museum of China, Mao et al. 2021) and *Jeholbaatar* (lower cheek teeth, IVPP V20778; modified from Wang et al. 2019); **b**. *Yubaatar zhongyuanensis* (41HIII0111, Henan Geological Museum, Zhengzhou, Henan Province, China; Xu et al. 2015); **c**. *Erythrobaatar* (GM30516; this study); **d**. *Taeniolabis taoensis* (upper cheek teeth, DMNH EPV.136300, left upper dentition, modified from Krause et al. 2021; lower cheek teeth, AMNH 16310, left lower dentition); **e**. *Lambdopsalis* (IVPP V5429; Chow and Qi 1978); **f**. *Ptilodus* (USNM V6076; Gidley 1909). The dotted curve lines indicate the premolar arc, the solid curve lines indicate the molar arc, and the stars indicate the turning point for the occlusal cycles of multituberculates. Abbreviations: **d**, deciduous; **L**, left; **M**, upper molar; **m**, lower molar; **P**, upper premolar; **p**, lower premolar; **R**, right. Images not to scale

process that extends anterolaterally; its anterior tip forms a blunt postorbital process that marks the posterodorsal end of the orbit. The temporal lines extend posterodorsally from the processes and merge at the anterior end of the sagittal crest. The posterior part of the parietal is short relative to the frontal in dorsal view, and bears a weak and short sagittal crest. The cranial vault is gently circular-arc shaped with the sagittal and nuchal crests intersecting at the peak of the arc.

In lateral view, no septomaxilla or internarial bar is found surrounding the nares, as in other multituberculates. The premaxilla and maxilla form the lateral wall of the rostrum. The lacrimal is strip-like and occupies the anteromedial margin of the orbit. Due to fractures the lacrimal foramen is not visible. The facial and zygomatic processes of the maxilla are laterally curved for a short distance and continue posteriorly to merge in the zygomatic arch. The leading edge of the zygomatic root displays a mild lateral extension so that the transition between the rostrum and zygoma is a gentle concavity. The single infraorbital foramen is small and located at the level above the junction between P3 and P4. The zygoma is slender for such a large cranium; it is long and of even thickness throughout its length. The jugal is a small and narrow laminar bone that clings to the inner surface of the anterior zygomatic arch. The jugal bridges the anterior portion of the suture between the zygomatic process of the maxilla and the squamosal. The parietal borders with the anterior lamina of the petrosal anteriorly and the squamosal posteriorly; the former makes up a large part of the braincase, whereas the latter forms the base of the zygoma and contributes to the lateral portion of the lambdoidal ridge.

In ventral view, the premaxillae form a small part of the palate. There are two pairs of upper incisors within the premaxilla. The incisive foramina are small within the premaxilla, but their boundary is not definite (not at the margin of the premaxilla) because of breakage in the area. The palatal portion between the incisive foramina and the palatal vacuity and between the latter and the cheek teeth are smooth and structureless. The maxillae form the main part of the palate. Two long, oval-shaped palatal vacuities are present in the middle of the palate; its anterior rim is level with P3 but its posterior extension is not certain due to breakage; it extends at least to the distal part of M1. The posterior part of the palate in the two specimens is broken so that the condition surrounding the choana is unknown except for the exposed presphenoid and vomer. The pterygoids project ventrally, forming a low crescent crest fused with the petrosal medial to the promontorium. The basicranial region is poorly preserved. Nonetheless, the surface of the promontorium appears relatively even and the size is small. The outline of the promontorium reflects the finger-like cochlea, which is confirmed by the cochlear recess exposed on both sides of the paratype specimen (GM30496). The deep and broad groove at the lateral side of the promontorium is the lateral trough but its precise limits are unclear. The fenestra vestibuli is oval in shape and posteromedially oriented on the lateral side of the promontorium. Posterior to the promontorium, the perilymphatic foramen opens into a sizable recess. As is typical for multituberculates, the glenoid fossa is oval in shape with a gently concave articular surface. The left occipital condyle is broken on its ventral part, whereas the right one is totally absent on the holotype.

In the occipital view, the supraoccipital, exoccipital, and basioccipital (the occipital condyle) are preserved from the dorsal to ventral. On the lateral sides of these bones is the large exposure of the petrosal that is pierced by the posttemporal canal in the middle.

Mandible Both dentary bones of the holotype are preserved in fairly good condition. The dentary is anteroposteriorly long and dorsoventrally shallow in depth (Fig. 4). The ventral border of the dentary is notably flat and the angle between the ventral margin of the dentary and the occlusal plane is lower than 15° or they are nearly parallel. The horizontal ramus is robust, but the ascending ramus is quite thin with its mediolateral width being a quarter of the horizontal ramus. The diastema between the incisor (at the distal edge of the alveolus) and p4 is long (11.78 mm); the part that contains the incisor is relatively long and slim because of a thin incisor. The dorsal edge of the diastema rises vertically to form the mesial wall of the alveolus of p4.

In lateral view, a small, round mental foramen is located immediately anterior to the p4 (Fig. 4b). The masseteric fossa is long and shallow, with a smooth gently concave surface, without sign of masseteric fovea; its deepest area is below m2. A ridge ascends from a level rear of the m1, continues posterodorsally, and joins with the coronoid process. Medial to the ridge is the deep and trough-like temporal groove (Gambaryan and Kielan-Jaworowska 1995). Posterior to the coronoid process, the masseteric fossa gradually fades away toward the mandibular condyle. The fossa is ventrally bounded by a crest that projects laterally, which is best seen in the dorsal view of the mandible. The extremity of the crest ends as the masseteric protuberance. The coronoid process is a triangular bony lamina that arises posterolateral to m2 and blocks most of m2 in lateral view. It is parallel with the sagittal plane of the horizontal ramus but has a small angle (12–15°) with the long axis of the dentition. In lateral view, its anterior edge is a gentle curve and has an angle of roughly 140° with the occlusal plane of the teeth. The posterior part of the process is broken but it is probable that the process ends with a pointed tip. The horizontal ramus continues posteriorly as the stem of the mandibular condyle. The stem is long and extends nearly horizontally, showing no dorsal turning. The transition from the coronoid process to the condyle is a smoothly concave edge. The condyle is low, with its dorsal edge barely leveling with the occlusal plane of the molars. The condyle is at the posterodorsal corner of the stem. The main articular surface is oval and transversely oriented; it tapers into a narrow strip while extending ventrally along the posterior end of the stem.

In lingual view, the symphysis is small, comma-shaped, and relatively smooth. The most conspicuous structure is the pterygoid ridge; it is a fan-shaped crest that projects medially and curves dorsomedially so that the ventral floor of

the pterygoid fossa forms a longitudinal trough that extends from m2 to the anteroventral area of the condyle. The mandibular foramen is large and opens in a deep pocket of the pterygoid fossa, posterior to m2.

Upper dentition The two type specimens are apparently from adult individuals with the cheek teeth being quite heavily worn (Fig. 5). There are two pairs of upper incisors of similar size within the premaxilla according to the holotype (GM30516); they are parallel to the lateral ventral edge of the premaxilla (Figs. 2 and 3). The I2 is placed along the lateral edge of the premaxilla, with the I3 positioned posterior to the I2 just inside and in parallel to the lateral margin of the premaxilla. The I2s are directed ventromedially toward each other but do not seem to contact each other medially and leave a triangular space between them. The I3s are placed on the palatal part but not the margin of the premaxilla. The right I3 is in a good condition; it is a long and conical tooth. A distinct diastema separates I3 from the mesial upper premolar in both specimens.

There are three upper premolars on each side of the maxilla identified as P2-P4 and P1 is absent entirely; all have two roots, as revealed by CT scan images (Fig. 7c). A small diastema exists between P2 and P3 in GM30496. Cusps of P2-3 are intact in at least one tooth and P2 is less worn than P3 in GM30496, whereas P4 is unquestionably the most heavily worn upper premolar. Thus, it may be inferred that the premolar eruption sequence proceeded distomesially or that the ultimate premolars were not replaced. The cusp formula of P2 is variable, with the cusp number of GM30516 being fewer than that of GM30496. The number is asymmetrical in GM30496: the cusp formula of the left P2 is 1:3 and the right one is 3:3. In contrast, the left P2 (the right one is broken) of GM30516 is 1:2. P3 is the smallest upper premolar. The cusp formula of P3 is 2:2 in GM30496, whereas in GM30496 there is an extra small cusp that adds to the distal end of the buccal row on each P3; thus, the buccal side projects distally. P4s of GM30496 were slightly displaced away from M1s, caused by the fracture of the maxilla. P4s of both specimens are worn, particularly on the lingual side. However, the crown shape of P4 is still discernable. It is mesiodistally long, about twice the length of P3 length, but is still small compared to the molars; the length ratio between P4 and M1, based on the right teeth of GM30516, is 0.513. A unique feature of P4 is that there is a restriction between the mesial and distal halves of the crown. In crown view, P4 is hourglass shaped in which the mesial portion, supported by a thinner root, is smaller than the distal one. The mesial portion consists of two closely packed lingual and buccal cusps. The mesiolingual portion of all P4s was worn away or broken; only the lateral sides of the buccal cusps are still discernable.

M1 is deeply worn in GM30516, which blurs the cusp shape and number. The right M1 of GM30496 is less worn. The cusp formula of M1 can be established as 7:7:5–6. M1 crown is trapeziform that slightly widens distally, mainly due to the addition of the lingual cusps that decrease mesially in size. The anterior portion of the lingual row is almost a narrow ridge that reaches the lingual side of cusp 1 in the middle row. The distal five cusps are well developed, comparable to those of the middle row in size, in which the penultimate cusp is the largest. Because of wear, the buccal side is lower than the lingual side for all lingual cusps. Each lingual cusp is positioned on the lingual side of the groove that transversely separates two neighboring cusps in the middle row. The middle cusp row is the lowest of the three, occupying the floor of the broad longitudinal valley created by wear. The outline of the worn cusp is square or rectangular, transversely wider, and each cusp is delimited by an enamel loop. Because of wear, the grooves separating neighboring cusps were gradually erased and the dentin of the two cusps becomes confluent.

The buccal cusps are taller than those of the middle rows partly because they are less worn; this is best seen in GM30496. The buccal cusps are transversely narrower than, and positioned in cusp-to-cusp with, those in the middle row, which contrasts with the cusp-to-groove relationship between the cusps of the lingual and middle rows. Opposite to the condition of the lingual row, the buccal side is higher than the lingual side for all buccal cusps because of wear. M1 develops two strong roots with multiple accessory roots like those in *Meniscoessus* and *Cimolomys* (Fig. 7).

M2 is almost as long as but notably wider than M1. M2 bears fewer cusps than M1, with a cusp formula of 2–3:4:4; its cusps are larger, more robust and less worn (the wear of M2 is still more extensive than that of most Cretaceous multituberculates) than those of M1. Both middle and lingual rows each consist of four cusps, while the buccal row has two main cusps with a minuscule cuspule being at the end of the row that ends buccal to cusp 3 in the middle row. Thus, the mesial half of the tooth crown is considerably wider than the distal half. Similar to other multituberculates, the arrangement of M2 cusp rows is one row lingually positioned relative to that of M1. M2 enamel is thicker and darker than M1. Two fusiform robust roots are anterior-posteriorly located.

The relatively elongated crown size of the molars, the strong main roots of molars and the multiple accessory roots of M1, and relatively extensive wear of molars compared to that of other Cretaceous multituberculates indicate that molars were primarily emphasized during the chewing cycle in *Erythrobaatar* (Fig. 7). This perhaps represents an evolutionary trend in taeniolabidoids that is characterized by a reduction of the premolars.

Lower dentition The sole lower incisor is blunt and procumbent (Fig. 4); it is relatively slim in relation to the size of

the dentary as well as compared to that of some cimolodontans, like djadochtatherians, other taeniolabidoids, microcosmodontids, eucosmodontids, etc. (Wible et al. 2019). As preserved,the slightly worn tip of the incisor is lower than the cheek tooth row and the wear facet on the tips is level to the middle part of the oblique occlusal plane of the cheek teeth. Enamel is restricted to the ventrolateral surface of the lower incisor, like the enamel of other taeniolabidoids (Mao et al. 2015). Because of the thick enamel, a fine groove is created along the lingual side of the enamel band. In cross-section the lower incisor is deeper than wide. The two incisors pair closely when the jaws are placed in presumed anatomical positions. The CT-image reveals that the root of the incisor extends distally to the level ventral to m1.

There are three cheek teeth in each lower jaw of GM30516. Of these teeth, the first molar shows the heaviest wear, as in the upper molars. The p4 is blade-like and transversely narrow. As for the upper teeth, p4 is much shorter than m1, with a length ratio of 0.685 (based on the right lower teeth of GM30516). The left p4 was longitudinally split into left and right halves in GM30516. Both p4s bear extensive wear on the buccal surfaces, showing that this is the occluding side of the tooth. The lingual surface bears no wear so it is convex with intact enamel. The right p4 of GM30516 has at least four blunt serrations but there is little sign of buccal or lingual ridges descending from them; the tooth profile is arcuate in buccal view.

Because of heavy wear, the cusp formula of m1 is difficult to ascertain. We estimate the m1 cusp formula as 7?:8?. The m1 is wider than p4 but narrower than m2. The m2 has four prominent cusps in each row that are followed by several conules at the ends of two rows. We interpret the cusp formula as 4–5:4–5. The lingual cusps are larger than the buccal ones. As in the upper molars, the m2 enamel is also thicker and darker than that of m1.

Comparison

Erythrobaatar ganensis is one of the largest Mesozoic cimolodontan multituberculates, only exceeded by the North American *Bubodens* (which is represented by a single molar) and maybe the Late Cretaceous *Yubaatar qianzhouensis* from southern China (which cranial width is 12% larger and m1 length is 25% larger but other teeth are smaller than that of *E. ganensis*, see Table 1). It has a cranium length of about 85 mm, which is smaller than the Paleocene *Taeniolabis taoensis* from North America (adult cranium length reaching 160mm, Granger and Simpson 1929; Krause et al. 2021). It is probably smaller than the Paleocene *Sphenopsalis* from the Mongolian Plateau, which has an M1-2 length of 29.7 mm (Mao et al. 2016), the Late Cretaceous *Bubodens magnus* (m1 dimensions of 12.8/6.0 mm) from North America (Wilson 1987), and the Paleocene *Boffius* (M1 dimensions of 15.0/9.0 mm) from Belgium (De Bast and Smith 2017).

Erythrobaatar is most similar to *Yubaatar* in its paleogeographical distribution, geological age, size, and morphology. The features that distinguish *Erythrobaatar ganensis* from *Yubaatar zhongyuanensis* Xu et al. (2015) are numerous, including: lack of P1; more cusps on m1-2 and M1-2; p4 shorter and less arcuate with fewer serrations; the zygomatic process slender and less laterally expanded; smaller angle between ventral margin of dentary and occlusal plane. *E. ganensis* further differs from *Y. qianzhouensis* Hu and Han (2021) in having a different cheek tooth cusp formula with more cusps on the molars in general (M2[2–3:4:4], m1[7?:8?], m2[5–6:4–5] in *E. ganensis*, M2[1:3:3], m1[7:6], m2[4:3] in *Y. qianzhouensis*); no posterobuccal cingulid on m1; M1 with multiple accessory roots; several conules developed at distal end of m2; molars larger (except m1s are remarkably shorter); the length radio of m2/m1 much larger; and the angle of lambdoidal ridges straighter.

Erythrobaatar is similar to *Yubaatar* in having the following craniodental features: p4 proportionally small and arcuate but not conical; molars not ornamented and cusps not coalesced; only one lower premolar; several accessory conules at the distal end of m2; the outline of cranium roughly square; parietal proportionally small whereas squamosal laterally extended; frontals are wedge-shaped and deeply wedged posteriorly between parietals; postorbital processes small; sizable palatal vacuity; dentary with small angle between ventral margin and occlusal plane. *Erythrobaatar* further resembles *Y. qianzhouensis* in that the small coronoid process is triangular in shape with a pointed tip.

Erythrobaatar and *Yubaatar* differ from other members of Taeniolabidoidea in several features: large palatal vacuity; lingual cusp row of M1 short; arcuate p4 transversely narrow with weak ridges rather than being conical; more upper premolars (three or four instead of only one premolar); larger, fewer cusps on upper and lower M1/m1; and small angle between ventral margin of dentary and occlusal plane.

Erythrobaatar and *Yubaatar* both are similar to the Late Cretaceous Mongolian *Buginbaatar* (*Buginbaatar transaltaiensis* Kielan-Jaworowska and Sochava, 1969) in lacking p3; having weak vertical, rather than oblique serrations on p4; low p4 crown and relatively small P4 in comparison with enlarged upper molars; lack of crescentic cusps on the molars; and m2 with fewer cusps. They differ from *Buginbaatar* in having shorter P4 and M1, more cusps on M2, and larger sizes of teeth.

Erythrobaatar differs from the Late Cretaceous Mongolian djadochtatherioids in that the cranium is square shape in dorsal view (vs. the gradual tapering from the zygomatic arches to the tip of the rostrum in djadochtatherioids), three premolars, more cusps on molars, smaller p4 that does not

Table 1 Comparison of Skull and dentition measurements (in mm) of *Erythrobaatar ganensis* gen. et sp. nov. with species of *Yubaatar*. The asterisk (*) denotes estimated measurement of preserved dimension of an element. Abbreviations: **L**, left; **R**, right

	E. ganensis GM30516 (length/width)	*E. ganensis* GM30496 (length/width)	*Yubaatar qianzhouensis* Hu and Han, 2021 41HIII0111 (length/width)	*Yubaatar zhongyuanensis* Xu et al., 2015 CUGW VH101 (length/width)
Skull length	84.81	78.81*	42.5*	70*
Maximum skull width	61.86	47.29*	70.2	
Dentary length (L)	61.26			56.6
Dentary length (R)	60.87			
I2	2.54/3.51 (L)	2.35/2.96 (L)		
I3	2.77/2.64 (R)	2.19/3.03 (L)		
P1 (L)				3.25/2.16
P2 (L)	3.49/3.01	2.44/2.02		2.95/2.27
P3 (L)	2.94/2.25	2.52/1.94		2.35/2.16
DP4				4.85/4.49
P4 (L)	5.06/2.20*	3.92/1.95		2.68/?
M1 (L)	10.47/5.54	7.20/3.73		9.5/4.75
M2 (L)	9.44/6.57	7.81/4.99		6.8/5.6
P2 (R)	3.65/2.05*	2.71/2.49		
P3 (R)	2.76/2.01	2.96/2.24		
P4 (R)	5.26/2.76	4.42/2.97		
M1 (R)	10.25/5.12			
M2 (R)	9.38/6.21		6.72/4.78	
i (R)	3.81/3.22			
p4 (R)	6.25/2.14			
m1 (R)	9.13/3.44			
m2 (R)	7.99/5.10			
i (L)	3.78/2.44			3.8/2.95
p4 (L)	6.338/?			6.97/2.23
m1 (L)	9.63/3.66		12.13*/4.16	9.2/3.58
m2 (L)	7.94/4.95		5.67*/?	6.7/5.14

protrude dorsally over the level of the molars, vertical, rather than oblique ridges on p4, square-shaped frontonasal suture rather than the V-shaped suture in djadochtatherioids, V-shaped frontoparietal suture rather than the rounded or square-shaped suture in djadochtatherioids, and shorter postglenoid region of the braincase relative to cranial length.

Erythrobaatar differs from the largest North American Cretaceous multituberculate *Bubodens* (Wilson 1987; Williamson et al. 2016) in that m1 is smaller in size with fewer cusps; the cusps are not compressed, lenticular, and crowded; and the enamel is not rugose. *Bubodens* was tentatively referred to Taeniolabidoidea because of its *Taeniolabis*-like morphology of inflated molar cusps with horizontal wear facets on the cusp tips (Kielan-Jaworowska et al. 2004). However, only m1 is known in this genus; Williamson et al. (2016) more recently tried to address the position of *Bubodens* within Taeniolabidoidea but a posteriori removed *Budodens* from the phylogenetic analysis to increase resolution; thus the affiliation of *Bubodens* is still uncertain.

Erythrobaatar differs from Cimolomyidae (*Cimolomys*, *Essonodon*, *Meniscoessus*, and *Paressonodon*) in having fewer premolars, a unicuspid upper incisor, fewer and blunt serrations on p4, molars not ornamented, cusps not coalesced, lingual cusp row of M1 shorter (not as long or almost as long as the other cusp rows), dentary slender and longer, and alveolar ridge weaker (Storer 1991; Weil and Tomida 2001; Wilson et al. 2010). *Erythrobaatar* differs from Microcosmodontidae in having a larger size, lower p4, and I3 placed on the palatal part but not at the margin of the premaxilla. *Erythrobaatar* differs from Kogainoidea in having larger size, different dental formula and cusp formula, shorter upper premolars, longer upper molars, p4 does not protrude dorsally over the level of the molars, wider snout, larger palatal vacuity, and the frontoparietal suture straight, not interdigitated.

Erythrobaatar differs from the *Paracimexomys* group (Kielan-Jaworowska et al. 2004) in having a larger size, different cusp formula, molars without coalescing cusps

and ornamentation, and P4 with two cusp rows equal in size. *Erythrobaatar* differs from Ptilodontoidea in having fewer premolars, a robust lower incisor covered with limited enamel band (not completely covered with enamel), smaller, less arcuate p4 that does not protrude dorsally over the level of the molars, I3 placed on the palatal part but not at the margin of the premaxilla, P4 shorter with fewer cusps, absence of ornamentation on the molars, and lack of molar cusp coalescence. *Erythrobaatar* differs from Eucosmodontidae in having larger size, unicuspid upper incisor, different cusp formula of cheek teeth, double-rooted P2-4, P4 short with two cusp rows (shorter than M1), and fewer serrations on p4, such as those of *Stygimys kuszmauli* Sloan and Van Valen, 1965 and *Stygimys cupressus* Fox, 1989).

Erythrobaatar differs from Arginbaataridae (Kielan-Jaworska et al. 1987), *Uzbekbaatar* (Kielan-Jaworowska and Nessov 1992), *Argentodites* (Kielan-Jaworowska et al. 2007) and Corriebaataridae (Rich et al. 2009) in having a larger size, less arcuate crown of p4 with one cusp row bearing vertical instead of oblique ridges, and lack of a buccal cuspule on p4. *Erythrobaatar* differs from Boffiidae Hahn and Hahn, 1983 in having a greater number of molar cusps, grooves, and ridges on P4 and M1.

Phylogeny

As mentioned in the methods, we performed phylogenetic analyses based on two datasets: Dataset I is modified after Wible et al. (2019) and includes 20 taxa and 121 characters focusing on relationships within Cimolodonta and Dataset II is modified after Smith et al. (2022) and includes 57 taxa and 130 characters and covers a wider range of multituberculates. The tree length of the strict consensus of the first analysis based on Dataset I is 352; the consistency index (CI) is 0.6364; the homoplasy index (HI) is 0.4858; the retention index (RI) is 0.6049; and the rescaled consistency index (RC) is 0.385. The tree length of the second analysis based on Dataset II is 559; the consistency index (CI) is 0.4508; the homoplasy index (HI) is 0.6351; the retention index (RI) is 0.7492; and the rescaled consistency index (RC) is 0.3377. For Dataset II, we discuss the phylogeny relationship based on Majority-rule consensus tree.

In both analyses based on datasets I and II, *Erythrobaatar* and *Yubaatar* are placed in a monophyletic Taeniolabidoidea (Fig. 8) according to the most recent definition for Taeniolabidoidea (Williamson et al. 2016: 200). However, in both analyses the relationships of

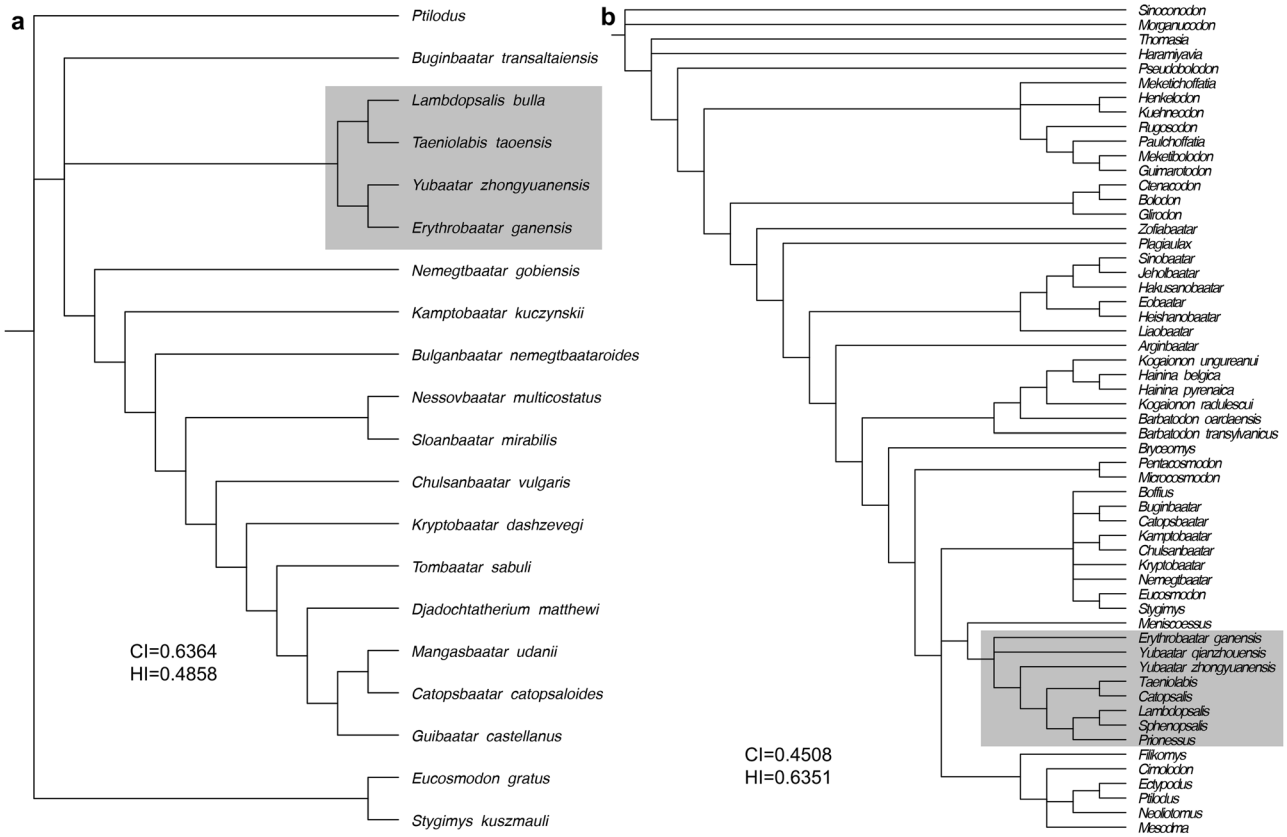

Fig. 8 Phylogenetic position of *Erythrobaatar ganensis* within multituberculates with focus on taeniolabidoids (gray box). **a**. strict consensus tree of three most parsimonious trees using dataset I; **b**. majority-rule consensus tree of two most parsimonious trees using dataset II

Taeniolabidoidea within Cimolodonta are unresolved. In analysis I, Taeniolabidoidea is placed in a polytomy with Djadochtatherioidea and Buginbaatar, and in analysis II, Taeniolabidoidea + *Meniscoessus* are resolved in a polytomy with Ptilodontidae and Djadochtatherioidea (plus *Eucosmodon*, *Stygimys*, and *Buginbaatar*).

The analysis based on dataset I pairs *Erythrobaatar* and *Yubaatar*, which in turn forms a sister group of the *Taeniolabis-Lambdopsalis* clade. In contrast, *Erythrobaatar ganensis*, *Yubaatar qianzhouensis*, and *Yubaatar zhongyuanensis* are placed as basal taxa within Taeniolabidoidea in the analysis based on dataset II. But in Dataset II, the tree shows that *Y. zhongyuanensis* is more closely related to other taeniolabidoids than to *Y. qianzhouensis* or *E. ganensis*. Also, *Y. qianzhouensis* and *E. ganensis* are in a polytomy at the base of that clade, so either are as closely related as the clade including *Y. zhongyuanensis* + Taeniolabidoidea as they are to each other.

In the first analysis, characters supporting the sister grouping of *Erythrobaatar* and *Yubaatar* include: enamel of lower incisor restricted to buccal surface of tooth; upper incisors are peg-like or single cusped; last upper premolar with two main, rows of cusps equal in length; number of upper postcanine loci fewer than five; m2 lingual row cusp count 4–5; lower m2 with buccal cusp row about equal in length to lingual cusp row; and upper M1 elongated. In analysis II, *Erythrobaatar* and *Yubaatar* are basal to the Cenozoic taeniolabidoids *Taeniolabis*, *Catopsalis*, *Lambdopsalis*, *Sphenopsalis* and *Prionessus*. Compared to those Cenozoic species, *Erythrobaatar* and *Yubaatar* display some plesiomorphic characters, such as having more upper premolars, molars shorter with fewer cusps, and molar cusps not specialized (either crescentic or blunt quadrate).

Most Cenozoic taeniolabidoids have specialized crescentic or blunt quadrate cusp morphologies, with the exception of the lambdopsalidan *Prionessus*. The apiciform to cone-shaped cusp morphology of *Prionessus* has previously been assumed to represent the ancestral condition for Taeniolabidoidea (Matthew et al. 1928; Mao et al. 2016). The deeply nested position of *Prionessus* and the basal position of *Erthyrobaatar* and *Yubaatar* within Taeniolabidoidea (that also have cone-shaped cups morphology) might further support that the apiciform to cone-shaped cusp morphology of *Prionessus*, *Erythrobaatar* and *Yubaatar* in fact represents the basal condition for Taeniolabidoidea. It is interesting that the Paleogene lambdopsalids *Lambdopsalis*, *Sphenopsalis*, and *Prionessus* from the Mongolian Plateau are only distantly related to the Late Cretaceous djadochtatherioidians that are also from the Mongolian Plateau. Instead they are more closely related to the North American Paleogene *Taeniolabis* and *Catopsalis* and the Late Cretaceous *Erythrobaatar* and *Yubaatar* from central China. These relationships suggest the dispersal event of the Taeniolabidoidea and Djadochtatherioidae may have happened earlier than the Late Cretaceous.

Discussion

P4/p4 replacement Based on comparisons of eruption patterns of multituberculates available at the time, Greenwald (1988) argued that the adult p4 of Late Cretaceous-Paleogene forms is homologous to the dp4 of diphyodont taxa such as the paulchoffatid *Kuehneodon dietrichi* (Hahn 1978), and pointed out that there is no evidence to support the replacement of upper P4 or lower p4 in multituberculates. Although Sloan (1981, 1987) argued that P4 was diphyodont in K-Pg multituberculates, this statement was not confirmed (Greenwald 1988). More recently, Xu et al. (2015) reported that the possible erupting P4 has a deciduous precursor that was heavily worn so that the last antemolar tooth is diphyodont and therefore a premolar, instead of a molar, in *Yubaatar*. Another reason that the tooth was identified as dP4 is that it was deeply worn, much more than M1. However, Xu et al. (2015) could not rule out other possibilities for the teeth in question. Juvenile specimens with evidence of two generations for premolar replacement of Cretaceous multituberculates are rare, if any; thus, whether the antemolar tooth at the P4 locus is diphyodont remains equivocal.

The specimens of *Erythrobaatar* provide no direct evidence about the premolar replacement. However, these specimens with associated upper and lower dentitions from the same individual animal that displays deep wear are not particularly common in the record of multituberculates. As in other mammals, the wear pattern is a good indicator of relative tooth eruptions in multituberculates (Greenwald 1988). The wears on the upper cheek teeth indicate that the first molar and the ultimate premolar functioned for a prolonged period before the second molar and the other premolars erupted and came into functioning. It is also unlikely that M1 was the first erupted cheek tooth and functioned alone before the ultimate premolar erupted, which was then followed by eruptions of P3 and P2 sequentially. From the wear pattern and known evidence of tooth replacement, it seems unlikely that the ultimate premolars of *Erythrobaatar* are successive teeth; unless their deciduous precursors were replaced in the early stage of ontogeny, earlier than the replacement of P3 and P2, which appears awkward and supported by no evidence.

It is worth mentioning that the crown of dP4 for *Yubaatar zhongyuanensis* is multicuspid and molariform, whereas the successive tooth of the dP4 is short and simple with fewer cusps (Xu et al. 2015; Fig. 7; unpublished CT data). The P4 shape of *Erythrobaatar* is comparable to the dP4 of *Yubaatar* but not the permanent P4. Based on our phylogenetic analyses and given the definition by Williamson

et al. (2016), *Yubaatar* and *Erythrobaatar* are basal taeniolabidoids. It is therefore reasonable to assume that P4s of *Erythrobaatar* are homologous to the dP4 of *Yubaatar*. As generally accepted that monophyodonty of various loci in mammals evolved through the suppression of secondary replacements for primary generation teeth (Ziegler 1971; Slaughter et al. 1974; McKenna 1975; Schwartz 1982), evidences of *Erythrobaatar* raise the possibility that the ultimate molariform upper premolar could be a deciduous tooth and its replacement pattern should be monophyodont.

Tooth reduction and homology As a rule, all multituberculates have two molars in each jaw quadrant, but their premolars vary greatly among various species. The general trend in the evolution of multituberculates is reduction of the antemolar cheek tooth number (Greenwald 1988). In the plesiomorphic Jurassic forms, the upper canine is present and there are up to five upper and four lower premolars (Kielan-Jaworowska et al. 2004). In the most advanced Cenozoic taeniolabidids, there are as few as only one premolar in each jaw quadrant (Krause et al. 2021). This general trend of tooth reduction can be seen in the clade of Taeniolabidoidea (Fig. 7). However, how the premolars were reduced and the tooth homologies resulting from the tooth reduction remain complicated (Clemens 1963; Hahn 1978; Kielan-Jaworowska and Hurum 2001). Within Cimolodonta, it is unclear how the upper premolars reduced from a four-tooth series to one tooth such as in our defined Taeniolabidoidea and how the lower premolars reduced from two to one small, peg-like tooth in derived taeniolabidoids.

For those cimolodontans that have four upper premolars, these teeth are closely packed and there is no diastema between any pair of teeth. There are, however, two configurations in tooth size that may be relevant to tooth reduction: P3 is the smallest premolar, such as in *Kamptobaatar* (Kielan-Jaworowska 1970, 1971), *Sloanbaatar* (Kielan-Jaworowska 1971), *Bulganbaatar*, and *Nemegtbaatar* (Kielan-Jaworowska 1974; Kielan-Jaworowska and Hurum 1997, 2001), or P2 is the smallest, such as in *Chulsanbaatar* (Kielan-Jaworowska 1974) and *Kryptobaatar* (Kielan-Jaworowska 1970; Wible and Rougier 2000; Smith et al. 2001). For those that have three upper premolars, there are also at least two configurations: a diastema exists between the first and second premolars, such as in *Catopsbaatar* (Kielan-Jaworowska et al. 2005), *Djadochtatherium* (Kielan-Jaworowska 1974), *Tombaatar* (Rougier et al. 1997), and *Mangasbaatar* (Rougier et al. 2016); or there is no diastema between any pair of the premolars, such as in *Guibaatar* (Wible et al. 2019). An inconsistent case is present in *Kamptobaatar*. In the reconstructed cranium of the genus, a well-developed diastema separates the mesial two premolars from the ultimate upper premolar (P4) (Wible et al. 2019: fig. 22E), whereas there are four premolars of *Kamptobaatar* in the original research, with the third one being the smallest (Kielan-Jaworowska 1971; Kielan-Jaworowska and Hurum 1997, 2001). As a result of these differences, the three premolars have been identified, for instance, as P1-P3-P4 for *Djadochtatherium* (Kielan-Jaworowska, 1974) and *Catopsbaatar* (Kielan-Jaworowska et al. 2005) or P2-P3-P4 for *Guibaatar* (Wible et al. 2019), which we tentatively follow in interpreting the premolars of *Erythrobaatar*, although we are not certain of the homology implied in those interpretations. It appears feasible that the P1-P3-P4 condition is derived from the four premolars with the smallest P2 lost so that a diastema is created at the P2 locus. Wible et al. (2019) speculated that the three premolars in the Late Cretaceous Mongolian multituberculates are homologous and the diastema in *Tombaatar*, *Catopsbaatar*, and *Mangasbaatar* is created by elongation of the rostrum during ontogeny, which occurred in adult individuals of large djadochtatheriids. However, as we report above, a small diastema exists between P2 and P3 in GM30496, which comes from an adult individual, whereas GM30516 represents an even older individual, judging from the tooth wear, and has a long rostrum; thus, absence of the alveolus within the upper premolar series may not be a result of ontogeny. We recommend that for those multituberculates that have three upper premolars, the homologies of P3 and P4 can be established, but the homology of the mesial premolar remains to be demonstrated.

How the three premolars, such as those in *Erythrobaatar*, were further reduced to the single premolar of derived taeniolabidoids is not very clear. However, *Erythrobaatar* possibly represents a transitional condition in tooth number and morphology from the Cretaceous form to the Cenozoic taeniolabidoids. *Erythrobaatar* differs from Djadochatherioidea (such as *Catopsbaatar*, *Djadochtatherium*, *Tombaatar*, *Mangasbaatar*, and *Guibaatar*) that have three upper premolars in having proportionally smaller upper and lower premolars. For the upper premolars, there is no record of a multituberculate that has two upper premolars; thus, from three premolars of some Late Cretaceous multituberculates, such as *Erythrobaatar*, to one premolar in the Cenozoic taeniolabidoids, there seems to be a morphological gap in terms of tooth number. Nonetheless, *Erythrobaatar* differs from Djadochatherioidea that have three upper premolars in that its premolars are proportionally small, or the molars are proportionally large.

The common pattern of lower premolars in cimolodontans consists of a peg-like or absent p3 and an enlarged and serrated blade-like p4 that shows a diverse morphology (Weaver and Wilson 2021). The sole p4 of *Erythrobaatar* is closely similar to the p4 of Cenozoic taeniolabidoids in being proportionally small relative to the enlarged molars. The evolution of basal cimolodontan multituberculates toward taeniolabidoids is quite different from those where the blade-like p4 became diversified (Kielan-Jaworowska et al. 2004; Wilson et al. 2012; Weaver and Wilson 2021);

instead, it emphasizes palinal chewing of molars for grinding so that the molars became enlarged and complex at the expense of the premolars and their function for slicing food; this trend can be further explored in the tooth occlusal relationship shown below.

Tooth occlusion Horizontal, palinal chewing has been considered a key feature of the earliest multituberculates, which differentiates them from "haramiyidans" (Butler and Hooker 2005; Averianov et al. 2021). The horizontal movement of the lower jaw in multituberculates is consistent with the molar structures that have straight cusp rows and furrows between them. However, if the cheek tooth row is viewed as a whole, the horizontal movement may only be a local phenomenon for the molars but not for the full mastication cycle that involves the full cheek tooth row. The shape of the tooth occlusal plane of the dentition may present physical constrain on the jaw movement. Krause (1982) established that the occlusion of multituberculates can be divided into two cycles: slicing-crushing essentially limited to the premolars, and grinding, essentially limited to the molars, which mainly focused on the functional aspect based on the wear on the tooth crown. Here, we mainly use the outline of the cheek tooth row in buccal view to emphasize the consistency of occlusion cycles during the evolution of multituberculates based on the new segmented CT data of several clades.

For multituberculates that have five or four upper premolars, the dentition generally shows two interesting features. The first one is that, in occlusal view, the cheek tooth row is usually arranged in a more or less curved course that is convex buccally, with the distal half of the ultimate premolar representing the outermost point of the curve. The occlusal line (running roughly along with the cusp tips) of the cheek tooth row is often flexuous in a broad "M"-shape (with the vertex located at the ultimate premolar). Here we use "occlusal line" rather than occlusal surface because this outline is not the actual occlusal surface in multituberculates. While the molar occlusion may follow this line, the premolar occlusion, particularly the ultimate pair of premolars, does not; p4 occludes on the ventral-lingual side of the ultimate premolar (Fig. 7; see Krause [1982: Fig. 10] for a different situation for *Ptilodus*); thus, the actual lower jaw movement is not in an M-shaped course. The anterior portion of the curved occlusal line is formed by the premolars, which we term the premolar arc, whereas the posterior portion is formed by the ultimate premolar and molars, which we term the molar arc. This flexuous pattern with two arcs is common in Jurassic and Cretaceous multituberculates where the upper dentition is known, such as the Late Jurassic paulchoffatiid *Henkelodon*, *Kuehneodon*, and *Pseudobolodon* (Hahn, 1977), Late Jurassic allodontid *Ctenacodon* (Bakker and Carpenter 1990), *Bolodon* (Kielan-Jaworowska et al. 1987), and many Cretaceous and Paleogene species (Krause 1982; Kielan-Jaworowska et al. 2004; Kusuhashi et al. 2009, 2020; Csiki-Sava et al. 2018; Wang et al. 2019; Mao et al. 2021; Weaver and Wilson 2021). This M-shaped occlusal line is illustrated by the upper cheek teeth of the Early Cretaceous *Sinobaatar pani* (Fig. 7a) in which the premolar arc ends in the middle of P5, whereas the posterior half of the P5 contributes to the molar arc (see also Kusuhashi et al. 2009). For those multituberculates that have four upper premolars, the vertex of the M-shaped occlusal line is on P4, as shown in *Yubaatar* (Fig. 7b); a similar pattern is present in other Late Cretaceous multituberculates, such as *Kryptobaatar*, *Kamptobaatar* (Kielan-Jaworowska 1970), and *Litovoi* (Csiki-Sava et al. 2018). In either the five or four premolar condition, the premolar and molar arcs usually are subequal in length (see Fig. 7a). The premolar arc in cimolodontans usually has an occlusal relationship with the enlarged p4 to function for the slicing-crushing cycle during mastication, whereas the molar arc functions for grinding (Hahn 1971; Krause 1982; Wall and Krause 1992; Weaver and Wilson 2021).

Erythrobaatar appears in a transitional stage between those with five or four upper premolars and derived taeniolabidoids. Owing to the reduction of one upper and lower premolar as well as shortening of the ultimate upper and lower premolars, the premolar arc is shortened to about half of the molar arc; the curvature of the arc is also reduced. The extremity of this premolar arc shortening is represented by Cenozoic taeniolabidoids in which there is only one peg-like ultimate premolar in both upper and lower jaws. As a result of this change, the upper cheek tooth row becomes short because the molars are the predominant functional teeth; accordingly, the premolar arc vanishes, whereas the molar arc is proportionally extended due to elongation of molars. Thus, in derived taeniolabidoids the slicing-crushing cycle of mastication, executed by the premolars, was essentially lost; only the grinding cycle of molars was retained and in fact, became enhanced (Krause 1982; Wilson et al. 2012; Weaver and Wilson 2021). This therefore probably indicates a dietary shift compared to those multituberculates that have two chewing cycles. However, as shown in the Cenozoic taeniolabidoids *Lambdopsalis, Sphenopsalis*, *Taeniolabis* (Mao et al., 2016) and *Kimbetopsalis* (Williamson et al. 2016), the occlusal line retains the gently curved (dorsally convex) molar arc. As such the palinal movement of the lower molars against the uppers follows a curvature and is not in a horizontal plane in Cenozoic taeniolabidoids. In contrast to the taeniolabidoid condition, ptilodontids evolved in a different direction by emphasizing the slicing-crushing cycle of mastication, as suggested by the hypertrophic p4 blade and the long upper premolar cycles which extends onto the mesial end of M1 (Krause 1982; Wall and Krause 1992; Weaver and Wilson 2021; Fig. 7f).

Finally, the occlusal relationship of teeth may furnish another criterion to infer tooth homologies of multituberculates. As noted by Butler (2000: 339): "the teeth must

continue to function throughout the evolutionary transformations of the body as a whole"; thus, the premolar and molar arcs of the cheek tooth row may support the hypothesis that P5 of primitive paulchoffatiids, plagaulacidans and eobaatarids is homologous to the tooth referred to as P4 in cimolodontans (Clemens 1963). In other words, the ultimate upper premolar, that forms the vertex of the M-shaped occlusal line between the premolar and molar arcs, is the dividing point between the distinct premolar-centric vs. molar-centric occlusal cycles. Similar function related to slicing-crushing and grinding cycles and relative position of 'P4' and P5 supports serial homology of the ultimate upper premolar in the evolution of cimolodontan multituberculates (Krause 1982).

Supplementary Information The online version contains supplementary material available at https://doi.org/10.1007/s10914-022-09636-2.

Acknowledgements We thank Shuhua Xie and Shijie Li (Institute of Vertebrate Paleontology and Paleoanthropology, Chinese Academy of Sciences, Beijing, China—IVPP) for specimen preparation; Yumao Hou, Pengfei Yin for CT scanning of the specimens; Wei Gao (IVPP) and Nicole Wong (American Museum of Natural History) for photography; Shengqun Lou (IVPP) for segmentation of the CT data; Qiang Wang (IVPP) for discussions concerning localities; Meng Chen (Nanjing University, Nanjing, China) and David W. Krause (Denver Museum of Nature and Science, Denver, USA) for sharing the scanning data of *Ptilodus* and *Taeniolabis taoensis*, respectively; David W. Krause, Lucas N. Weaver (University of Michigan), and Simone Hoffmann (New York Institute of Technology) for their insights and helpful comments; Simone Hoffmann and Darin Croft (Journal of Mammalian Evolution) for constructive editorial efforts.

Funding This work was supported by the National Natural Science Foundation of China (41404022; 42122010; 41688103), the Youth Innovation Promotion Association CAS (2019076); and the Kalbfleisch Fellowship, Richard Gilder Graduate School, American Museum of Natural History.

Data availability The phylogenetic datasets generated and/or analyzed during the current study are available in the Morphobank repository: http://morphobank.org/permalink/?P4398. The CT datasets generated and/or analyzed during the current study are not publicly available due to ongoing work on multituberculate skeletal anatomy but are available from the corresponding author upon reasonable request.

Declarations

Competing interest The authors declare that they have no competing interest.

References

Averianov AO, Martin T, Lopatin AV, Schultz JA, Schellhorn R, Krasnolutskii S, Skutschas P, Ivantsov S (2021) Multituberculate mammals from the Middle Jurassic of Western Siberia, Russia, and the origin of Multituberculata. Pap Palaeontol 7:769-787. https://doi.org/10.1002/spp2.1317

Bakker RT, Carpenter K (1990) A new latest Jurassic vertebrate fauna, from the highest levels of the Morrison Formation at Como Bluff, Wyoming. Part III. The mammals: a new multituberculate and new paurodont. Hunteria 2:4-8

Butler PM (2000) Review of the early allotherian mammals. Acta Palaeontol Pol 45:317-342

Butler PM, Hooker JJ (2005) New teeth of allotherian mammals from the English Bathonian, including the earliest multituberculates. Acta Palaeontol Pol 50:185-207

Bureau of Geology and Mineral Resources of Jiangxi Province (1984) Regional Geology and of Jiangxi Province. Geological Publishing House, Beijing

Cheng Y-N, Ji Q, Wu X-C, Shan H-Y (2008) Oviraptorosaurian eggs (Dinosauria) with embryonic skeletons discovered for the first time in China. Acta Geol Sin 82:1089-1094. https://doi.org/10.1111/j.1755-6724.2008.tb00708.x

Chow M, Qi T (1978) Paleocene mammalian fossils from Nomogen Formation of Inner Mongolia. Vert PalAsiat 16:77-85

Cifelli RL, Gordon CL, Lipka TR (2013) New multituberculate mammal from the Early Cretaceous of eastern North America. Can J Earth Sci 50:315-323. https://doi.org/10.1139/e2012-05

Clemens WA Jr (1963) Fossil mammals of the type Lance Formation. Part I. Introduction and Multituberculata. University of California Press, Oakland

Cope ED (1884) The Tertiary Marsupialia. Am Nat 18:686-697. https://doi.org/10.1086/273711

Csiki-Sava Z, Vremir M, Meng J, Brusatte SL, Norell MA (2018). Dome-headed, small-brained island mammal from the Late Cretaceous of Romania. Proc Natl Acad Sci USA 115:4857-4862. https://doi.org/10.1073/pnas.1801143115

De Bast E, Smith T (2017) The oldest Cenozoic mammal fauna of Europe: implication of the Hainin reference fauna for mammalian evolution and dispersals during the Paleocene. J Syst Palaeontol 15:741-785. https://doi.org/10.1080/14772019.2016.1237582

Fox RC (1989) The Wounded Knee local fauna and mammalian evolution near the Cretaceous-Tertiary boundary, Saskatchewan, Canada. Palaeontogr Abt A 208:11-59

Fox RC (2005) Microcosmodontid multituberculates (Allotheria, Mammalia) from the Paleocene and Late Cretaceous of western Canada. Palaeontogr Canadiana 23:1-109

Gambaryan PP, Kielan-Jaworowska Z (1995) Masticatory musculature of Asian taeniolabidoid multituberculate mammals. Acta Palaeontol Pol 40:45-108

Gidley JW (1909) Notes on the fossil mammalian genus *Ptilodus* with descriptions of new species. Proc US Natl Mus 293:611-626

Granger W, Simpson GG (1929) A revision of the Tertiary Multituberculata. Bull Am Mus Nat Hist 56:601-676

Greenwald NS (1988) Patterns of tooth eruption and replacement in multituberculate mammals. J Vertebr Paleontol 8:265-277. https://doi.org/10.1080/02724634.1988.10011709

Hahn G (1971) The dentition of the Paulchoffatiidae (Multituberculata, upper Jurassic). Mem Serv Geol Port 17:7-39

Hahn G (1977) Neue Schädel-Reste von Multituberculaten (Mammalia) aus dem Malm Portugals. Geol Paleontol 11:161-186

Hahn G (1978) Milch-Bezahnungen von Paulchoffatiidae (Multituberculata; Ober-Jura). Neues Jahrb Geol Palaeontol 1978:25-34

Hahn G, Hahn R (1983) Multituberculata. In: Westphal F (ed) Fossilium Catalogus, I: Animalia, Pars 127. Kugler Publications, Amsterdam, pp 1-409

He FL, Huang XJ, Li XY (2017) Occurrence rule and buried characteristics of dinosaur fossils in the Ganzhou Basin, Jiangxi Province. East China Geol 38:250–254. https://doi.org/10.16788/j.hddz.32-1865/P.2017.04.002

Hu JF, Han FL (2021) A new multituberculate, *Yubaatar qianzhouensis* sp. nov.: the first Late Cretaceous mammal from Ganzhou Basin, Jiangxi Province. Acta Palaeontol Sinica 60:2020057. https://doi.org/10.19800/j.cnki.aps.2020057

Jin XS, Varricchio DJ, Poust AW, He T (2020) An oviraptorosaur adult-egg association from the Cretaceous of Jiangxi Province, China. J Vertebr Paleontol 39:e1739060. https://doi.org/10.1080/02724634.2019.1739060

Kielan-Jaworowska Z (1970) New Upper Cretaceous multituberculate genera from Bayn Dzak, Gobi Desert. Palaeontol Pol 21:35-49

Kielan-Jaworowska Z (1971) Skull structure and affinities of the Multituberculata. Palaeontol Pol 25:5-41

Kielan-Jaworowska Z (1974) Multituberculate Succession in the Late Cretaceuos of the Gobi Desert (Mongolia). Palaeontol Pol 30:23-44

Kielan-Jaworowska Z, Cifelli RL, Luo Z-X (2004) Mammals from the Age of Dinosaurs: Origins, Evolution, and Structure. Columbia University Press, New York, NY

Kielan-Jaworowska Z, Dashzeveg D, Trofimov BA (1987) Early Cretaceous multituberculates from Mongolia and a comparison with Late Jurassic forms. Acta Palaeontol Pol 32:3-47

Kielan-Jaworowska Z, Hurum JH (1997) Djadochtatheria-a new suborder of multituberculate mammals. Acta Palaeontol Pol 42:201-242

Kielan-Jaworowska Z, Hurum JH (2001) Phylogeny and systematics of multituberculate mammals. Palaeontology 44:389-429. https://doi.org/10.1111/1475-4983.00185

Kielan-Jaworowska Z, Hurum JH, Lopatin AV (2005) Skull structure in *Catopsbaatar* and the zygomatic ridges in multituberculate mammals. Acta Palaeontol Pol 50:487-512

Kielan-Jaworowska Z, Nessov LA (1992) Multituberculate mammals from the Cretaceous of Uzbekistan. Acta Palaeontol Pol 37:1-17

Kielan-Jaworowska Z, Ortiz-Jaureguizar E, Vieytes C, Pascual R, Goin FJ (2007) First ?cimolodontan multituberculate mammal from South America. Acta Palaeontol Pol 52:257-262

Kielan-Jaworowska Z, Sochava AV (1969) The first multituberculate from the uppermost Cretaceous of the Gobi Desert (Mongolia). Acta Palaeontol Pol 14:355-367

Krause DW (1982) Jaw movement, dental function, and diet in the Paleocene multituberculate *Ptilodus*. Paleobiology 8:265-281. https://doi.org/10.1017/S0094837300006989

Krause DW, Hoffmann S, Lyson TR, Dougan LG, Petermann H, Tecza A, Chester SGB, Miller IM (2021) New skull material of *Taeniolabis taoensis* (Multituberculata, Taeniolabididae) from the early Paleocene (Danian) of the Denver Basin, Colorado. J Mamm Evol 28:1083-1143. https://doi.org/10.1007/s10914-021-09584-3

Krishtalka L, Emry RJ, Storer JE, Sutton JF (1982) Oligocene multituberculates (Mammalia: Allotheria): youngest known record. J Paleontol 56:791-794

Kusuhashi N, Hu Y-M, Wang Y-Q, Setoguchi T, Matsuoka H (2009) Two eobaatarid (Multituberculata; Mammalia) genera from the Lower Cretaceous Shahai and Fuxin formations, northeastern China. J Vertebr Paleontol 29:1264-1288. https://doi.org/10.1671/039.029.0433

Kusuhashi N, Wang Y-Q, Jin X (2020) A new eobaatarid multituberculate (Mammalia) from the Lower Cretaceous Fuxin Formation, Fuxin-Jinzhou Basin, Liaoning, northeastern China. J Mamm Evol 27:605-623. https://doi.org/10.1007/s10914-019-09481-w

Li C, Wu X-C, Rufolo SJ (2019) A new crocodyloid (Eusuchia: Crocodylia) from the Upper Cretaceous of China. Cretaceous Res 94:25-39. https://doi.org/10.1016/j.cretres.2018.09.015

Liu YG (1997) The Lithostratigraphy of Jiangxi Province. China Universtiy of Geosciences Press, Wuhan.

Liu YG (1999) Classification and stratigraphic positon of dinosaurian eggs in Jiangxi. Jiangxi Geol 13:3-7

Linnaeus C (1758) Systema naturae per regna tria naturae, secundum classes, ordines, genera, species, cum characteribus, differentiis, synonymis, locis. Vol. 1: Regnum animale. Editio decimal reformata. Laurentii Salvii, Stockholm

Lü J, Chen R, Brusatte SL, Zhu Y, Shen C (2016) A Late Cretaceous diversification of Asian oviraptorid dinosaurs: evidence from a new species preserved in an unusual posture. Sci Rep 6:35780. https://doi.org/10.1038/srep35780

Lü J, Ji S, Dong Z, Wu X (2008) An Upper Cretaceous lizard with a lower temporal arcade. Naturwissenschaften 95:663-669. https://doi.org/10.1007/s00114-008-0364-1

Lü J, Pu H, Kobayashi Y, Xu L, Chang H, Shang Y, Liu D, Lee Y-N, Kundrát M, Shen C (2015) A new oviraptorid dinosaur (Dinosauria: Oviraptorosauria) from the Late Cretaceous of southern China and its paleobiogeographical implications. Sci Rep 5:11490. https://doi.org/10.1038/srep11490

Lü J, Yi L, Brusatte SL, Yang L, Li H, Chen L (2014) A new clade of Asian Late Cretaceous long-snouted tyrannosaurids. Nat Commun 5:3788. https://doi.org/10.1038/ncomms4788

Lü J, Yi L, Zhong H, Wei X (2013a) A new oviraptorosaur (Dinosauria: Oviraptorosauria) from the Late Cretaceous of southern China and its paleoecological implications. PLoS One 8:e80557. https://doi.org/10.1371/journal.pone.0080557

Lü J, Yi L, Zhong H, Wei X (2013b) A new somphospondylan sauropod (Dinosauria, Titanosauriformes) from the Late Cretaceous of Ganzhou, Jiangxi Province of southern China. Acta Geol Sinica 87:678-685. https://doi.org/10.1111/1755-6724.12079

Lucas SG (2001) Chinese Fossil Vertebrates. Columbia University Press, New York.

Luo Z-X, Kielan-Jaworowska Z, Cifelli RL (2002) In quest for a phylogeny of Mesozoic mammals. Acta Palaeontol Pol 47:1-78

Mao F-Y, Liu C-Y, Chase MH, Smith AK, Meng J (2021) Exploring ancestral phenotypes and evolutionary development of the mammalian middle ear based on Early Cretaceous Jehol mammals. Natl Sci Rev 8:nwaa188. https://doi.org/10.1093/nsr/nwaa188

Mao F-Y, Wang Y-Q, Meng J (2015) A systematic study on tooth enamel microstructures of *Lambdopsalis bulla* (Multituberculate, Mammalia) - implications for multituberculate biology and phylogeny. PloS One 10:e0128243. https://doi.org/10.1371/journal.pone.0128243

Mao F-Y, Wang Y-Q, Meng J (2016) New specimens of the multituberculate mammal *Sphenopsalis* from China: implications for phylogeny and biology of taeniolabidoids. Acta Palaeontol Pol 61:429-454. https://doi.org/10.4202/app.00117.2014

Marsh OC (1880) Notice on Jurassic mammals representing two new orders. Am J Sci 20:235-239

Matthew WD, Granger W, Simpson GG (1928) Paleocene multituberculates from Mongolia. Am Mus Novit 331:1-4

McKenna MC (1975) Toward a phylogenetic classification of the Mammalia. In: Luckett WP, Szalay FS (eds) Phylogeny of the Primates. Plenum Press, New York, pp 21-46

Miao D-S (1988) Skull morphology of *Lambdopsalis bulla* (Mammalia, Multituberculata) and its implications to mammalian evolution. Contrib Geol Univ Wyoming Spec Pap 4:1-104

Mo JY, Xu X (2015) Large theropod teeth from the Upper Cretaceous of Jiangxi, southern China. Vert PalAsiat 53:63-72

Mo JY, Xu X, Evans SE (2012) A large predatory lizard (Platynota, Squamata) from the Late Cretaceous of South China. J Syst Palaeontol 10:333-339. https://doi.org/10.1080/14772019.2011.588254

Mo JY, Xu X, Susan EE (2010) The evolution of the lepidosaurian lower temporal bar: new perspectives from the Late Cretaceous of South China. Proc Roy Soc B 277:331-336. https://doi.org/10.1098/rspb.2009.0030

Novacek MJ, Norell M, McKenna MC, Clark J (1994) Fossils of the Flaming Cliffs. Sci Am 271:60-69

Rădulescu C, Samson PM (1996) The first multituberculate skull from the Late Cretaceous (Maastrichtian) of Europe (Haţeg Basin, Romania). Anu Inst Geol Românei 69:177-178

Rich TH, Vickers-Rich P, Flannery TF, Kear BP, Cantrill DJ, Komarower P, Kool L, Pickering D, Trusler P, Morton S (2009).

An Australian multituberculate and its palaeobiogeographic implications. Acta Palaeontol Pol 54:1-6. https://doi.org/10.4202/app.2009.0101

Rougier GW, Novacek MJ, Dashzeveg D (1997) A new multituberculate from the Late Cretaceous locality Ukhaa Tolgod, Mongolia: considerations on multituberculate interrelationships. Am Mus Novit 3191:1-26

Rougier GW, Sheth AS, Spurlin BK, Bolortsetseg M, Novacek MJ (2016) Craniodental anatomy of a new Late Cretaceous multituberculate mammal from Udan Sayr, Mongolia. Palaeontol Pol 67:197-248. https://doi.org/10.4202/pp.2016.67_197

Sato T, Cheng Y-N, Wu X-C, Zelenitsky DK, Hsiao Y-F (2005) A pair of shelled eggs inside a female dinosaur. Science 308:375-375. https://doi.org/10.1126/science.1110578

Schwartz JH (1982) Morphological approach to heterodonty and homology. In: Kurten B (ed) Teeth: Form, Function, and Evolution. Columbia University Press, New York, pp 123-144

Simmons NB (1993) Phylogeny of Multituberculata. In: Szalay FS, Novacek MJ, McKenna MC (eds) Mammal Phylogeny: Mesozoic Differentiation, Multituberculates, Monotremes, Early Therians, and Marsupials. Springer Verlag, New York, pp 146-164

Slaughter BH, Pine RH, Pine NE (1974) Eruption of cheek teeth in Insectivora and Carnivora. J Mammal 55:115-125. https://doi.org/10.2307/1379261

Sloan RE, Van Valen L (1965) Cretaceous mammals from Montana. Science 148:220-227. https://doi.org/10.1126/science.148.3667.220

Sloan RE (1979) Multituberculata. In: Fairbridge RW, Jablonski D (eds) The Encyclopedia of Paleontology. Dowden, Hutchinson & Ross, Stroudsberg, pp 492–498

Sloan RE (1981) Systematics of Paleocene multituberculates from the San Juan Basin, New Mexico. In: Lucas SJ, Rigby JJK, Kues BS (eds) Advances in San Juan Basin Paleontology. University of New Mexico Press, Albuquerque, pp 127-160

Sloan RE (1987) Paleocene and latest Cretaceous mammal ages, biozones, magnetozones, rates of sedimentation, and evolution. Geol Soc Am Spec Pap 209:165-200

Smith T, Codrea V (2015) Red iron-pigmented tooth enamel in a multituberculate mammal from the Late Cretaceous Transylvanian "Haţeg island". PLoS One 10:e0132550. https://doi.org/10.1371/journal.pone.0132550

Smith T, Codrea VA, Devillet G, Solomon AA (2022) A new mammal skull from the Late Cretaceous of Romania and phylogenetic affinities of kogaionid multituberculates. J Mammal Evol 29:1-26. https://doi.org/10.1007/s10914-021-09564-7

Smith T, Guo D-Y, Sun Y (2001) A new species of *Kryptobaatar* (Multituberculata): the first Late Cretaceous mammal from Inner Mongolia (PR China). Bull Inst Roy Sci Nat Belg Sci Terre, Suppl 71:29-50

Storer JE (1991) The mammals of the Gryde Local Fauna, Frenchman Formation (Maastrichtian: Lancian), Saskatchewan. J VertebrPaleontol 11:350-369. https://doi.org/10.1080/02724634.1991.10011403

Swisher III CC, Prothero DR (1990) Single-crystal 40Ar/39Ar dating of the Eocene-Oligocene transition in North America. Science 249:760-762. https://doi.org/10.1126/science.249.4970.760

Swofford DL (2002) Phylogenetic Analysis Using Parsimony, Version 4.0b10. Sinauer Associates, Inc., Sunderland, MA

Tong H, Mo J (2010) *Jiangxichelys*, a new nanhsiungchelyid turtle from the Late Cretaceous of Ganzhou, Jiangxi Province, China. Geol Mag 147:981-986. https://doi.org/10.1017/S0016756810000671

Tong YS, Wang JW (2006) Fossil mammals from the early Eocene Wutu formation of Shandong Province. Palaeontol Sinica, NS C 192:1-195

Wall CE, Krause DW (1992) A biomechanical analysis of the masticatory apparatus of *Ptilodus* (Multituberculata). J Vertebr Paleontol 12:172-187. https://doi.org/10.1080/02724634.1992.10011448

Wang HB, Meng J, Wang YQ (2019) Cretaceous fossil reveals a new pattern in mammalian middle ear evolution. Nature 576:102-105. https://doi.org/10.1038/s41586-019-1792-0

Wang S, Sun C, Sullivan C, Xu X (2013). A new oviraptorid (Dinosauria: Theropoda) from the Upper Cretaceous of southern China. Zootaxa 3640:242–257. https://doi.org/10.11646/zootaxa.3640.2.7

Wang S, Zhang S, Sullivan C, Xu X (2016) Elongatoolithid eggs containing oviraptorid (Theropoda, Oviraptorosauria) embryos from the Upper Cretaceous of Southern China. BMC Evol Biol 16:1-21. https://doi.org/10.1186/s12862-016-0633-0

Weaver LN, Varricchio DJ, Sargis EJ, Chen M, Freimuth WJ, Mantilla GPW (2021) Early mammalian social behaviour revealed by multituberculates from a dinosaur nesting site. Nat Ecol Evol 5:32-37. https://doi.org/10.1038/s41559-020-01325-8

Weaver LN, Wilson GP (2021) Shape disparity in the blade-like premolars of multituberculate mammals: functional constraints and the evolution of herbivory. J Mammal 102:967-985. https://doi.org/10.1093/jmammal/gyaa029

Wei X, Pu H, Xu L, Liu D, Lü J (2013) A new oviraptorid dinosaur (Theropoda: Oviraptorosauria) from the Late Cretaceous of Jiangxi Province, southern China. Acta Geol Sinica 87:899-904. https://doi.org/10.1111/1755-6724.12098

Weil A (1998) A new species of *Microcosmodon* (Mammalia: Multituberculata) from the Paleocene Tullock Formation of Montana, and an argument for the Microcosmodontinae. PaleoBios 18(2-3):1–15

Weil A, Krause DW (2008) Multituberculata. In: Janis CM, Gunnell GF, Uhen MD (eds) Evolution of Tertiary Mammals of North America, Volume 2: Small Mammals, Xenarthrans, and Marine Mammals. Cambridge University Press, Cambridge, pp 19-38

Weil A, Tomida Y (2001) First description of the skull of *Meniscoessus robustus* expands known morphological diversity of Multituberculata and deepens phylogenetic mystery. J Vertebr Paleontol 21:112A

Wible JR, Rougier GW (2000) Cranial anatomy of *Kryptobaatar dashzevegi* (Mammalia, Multituberculata), and its bearing on the evolution of mammalian characters. Bull Am Mus Nat Hist 247:1-120. https://doi.org/10.1206/0003-0090(2000)247<0001:CAOKDM>2.0.CO;2

Wible J R, Shelley SL, Bi S (2019) New genus and species of djadochtatheriid multituberculate (Allotheria, Mammalia) from the Upper Cretaceous Bayan Mandahu Formation of Inner Mongolia. Ann Carnegie Mus 85:285-327. https://doi.org/10.2992/007.085.0401

Williamson TE, Brusatte SL, Secord R, Shelley S (2016) A new taeniolabidoid multituberculate (Mammalia) from the middle Puercan of the Nacimiento Formation, New Mexico, and a revision of taeniolabidoid systematics and phylogeny. Zool J Linn Soc 177:183-208. https://doi.org/10.1111/zoj.12336

Wilson GP, Dechesne M, Anderson IR (2010) New latest Cretaceous mammals from northeastern Colorado with biochronologic and biogeographic implications. J Vertebr Paleontol 30:499-520. https://doi.org/10.1080/02724631003620955

Wilson GP, Evans AR, Corfe IJ, Smits PD, Fortelius M, Jernvall J (2012) Adaptive radiation of multituberculate mammals before the extinction of dinosaurs. Nature 483:457-460. https://doi.org/10.1038/nature10880

Wilson RW (1987) Late Cretaceous (Fox Hills) multituberculates from the Red Owl Local Fauna of western South Dakota. Dakoterra 3:118-132

Xing L, Niu K, Ma W, Zelenitsky DK, Yang T-R, Brusatte SL (2021) An exquisitely preserved in-ovo theropod dinosaur embryo sheds light on avian-like prehatching postures. iScience 25:103516. https://doi.org/10.1016/j.isci.2021.103516

Xu X, Han FL. 2010. A new oviraptorid dinosaur (Theropoda: Oviraptorosauria) from the Upper Cretaceous of China. Vert PalAsiat 48:11-18

Xu L, Zhang X, Pu H, Jia S, Zhang J, LüJ, Meng J (2015) Largest known Mesozoic multituberculate from Eurasia and implications

for multituberculate evolution and biology. Sci Rep 5:14950. https://doi.org/10.1038/srep14950

Young CC (1965) Fossil eggs from Nanhsiung, Kwangtung and Kanchou, Kianhsi. Vert PalAsiat 2:159-189

Young CC (1973) A Cretaceous lizard from Ganxian, Jiangxi. Vert PalAsiat 11:44-45.

Yuan C-X, Ji Q, Meng Q-J, Tabrum AR, Luo Z-X (2013) Earliest evolution of multituberculate mammals revealed by a new Jurassic fossil. Science 341:779-783. https://doi.org/10.1126/science.1237970

Zhao ZK (1975) The microstructure of dinosaurian eggshells of Nanhsiung Basin, Guangdong Province. Vert PalAsiat 13:105-117

Zhao ZK (1979) The advancement of research on the dinosaurian eggs in China. In: NGPIIa (ed) Mesozoic and Cenozoic red beds in Southern China. Science Press, Beijing, pp 330–340

Zhao ZK, Ye J, Li HM, Zhao ZH, Yan Z (1991) Extinction of the dinosaurs across the Cretaceous-Tertiary boundary in Nanxiong Basin, Guangdong Province. Vert PalAsiat 29:1-20

Zhong CT, Xu P, Xiao XL, Wang DW, Long T (2002) Revision of the Late Cretaceous Maodian Formation of the Ganzhou Group in Jiangxi Province. Geol China 29:271-274

Ziegler AC (1971) A theory of the evolution of therian dental formulas and replacement patterns. Quart Rev Biol 46:226-249